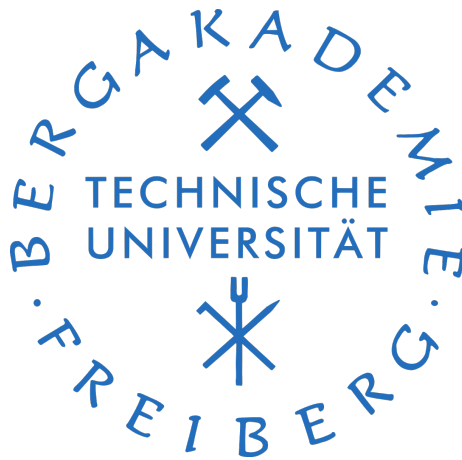# Development and implementation of material subroutine for fibre reinforced plastics in a commercial FEM software

Master thesis

Winter semester 2018/19

Presented by: Arun prakash Ganapathy

Supervised by: Dr.-Ing Dominik Laveuve

Mat.Nr: 63876

E-mail: arun-prakash.ganapathy@student.tu-freiberg.de

0.1 Introduction

0.1.1 Background and motivation

Composite materials are made of two or more dissimilar materials of different physical or chemical properties when combined, create a material with properties unlike the individual constituent materials. The earliest use of composite materials date back to 3400 B.C when Mesopotamians glued wood strips at different angles to create plywood. Another notable example is the bow made by Mongols during 1200 A.D, which is made from a combination of bamboo, wood, cattle tendons and silk bonded with natural resin. In the early, 1900s bakelite based composites were developed for its non-conductivity and heat resistant properties and widely used in industrial and consumer applications. Now a days advanced composite materials are widely used in structural design in various industries such as aerospace, automobile, marine, petrochemical etc., due to their superior properties over traditional engineering materials.
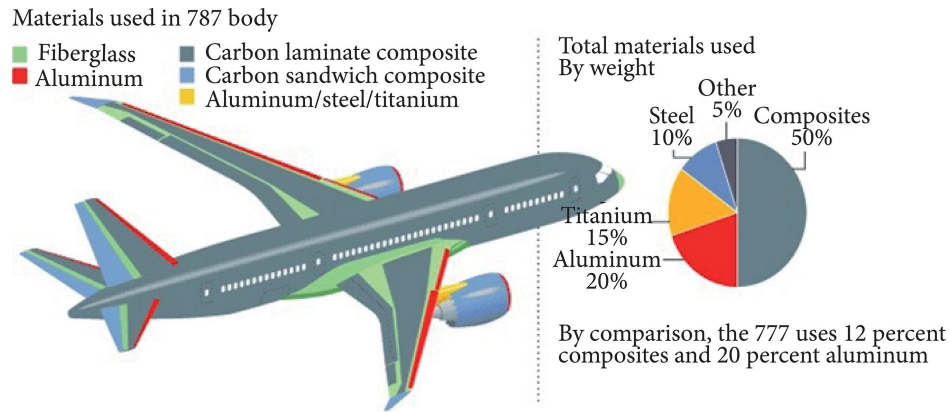

Figure 1: Composite materials used in a Boeing 787 'Dreamliner'

Composite material are attractive because of their high strength, stiffness, high stiffness-to-density ratio, light weight properties etc., Another important reason for using composite materials is the ability to tailor the stiffness and strength to specific design load flexibly. Despite their superior physical properties, composite materials are fragile and can be easily damaged from number of sources, both during initial processing and in operation. Since composite materials possess elastic brittle properties with negligible margin of safety through ductility as offered by metals and accumulate damage before structural collapse, the development of damage must be understood for predicting failure of such materials. For example fibre-reinforced plastics exhibit local damage such as fibre breakage, matrix cracks, fibre matrix debonds etc., under normal operating conditions which may contribute to the failure. Therefore the ability to predict the initiation and growth of damage is important for predicting the performance of the

composite materials for safe and reliable use of such materials. Continuum damage mechanics (CDM) has been considered as a reliable candidate for creating numerical models which predict the onset and evolution of the damage in the composite materials.

0.2　Continuum damage mechanics

Continuum damage mechanics (CDM) is a theory for analyzing damage and fracture processes in materials from continuum mechanics point of view. Continuum damage mechanics (CDM) provides a continuum perspective for microflaws initiation, propagation, and their coalescence that eventually results in macroscopic faults and fractures. CDM uses state variables to represent the effect of damage on the stiffness and remaining life of the material that is damaging as a result of load and ageing. A Damage activation function is required to predict the initiation of damage. Damage evolution does not progress spontaneously after initiation therefore a mathematical model is required.

0.2.1　Damage

Consider a body B of Fig. 2 where a crack of length a has developed due to an external load F. If we take an arbitrary point $P(x)$ near the crack tip, a number of microscopic cavities or microcracks would be observed around the region. These cavities can be nucleated usually as a result of breakage of atomic bonds, or of some defects in atomic array. From microscopic point of view, fracture of materials is a process of nucleation of microcavities or microcracks due to the breakage of atomic bonds. From macroscopic point of view, it is a process of extension of cracks brought about by the coalescence of these microcracks. From mesoscopic point of view, which
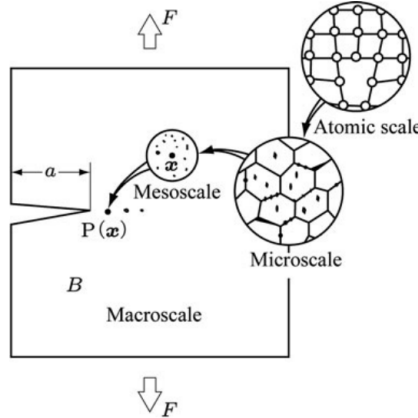

Figure 2: Scales of damage observation

exists between microscopic and macroscopic scale, it is a process of nucleation, growth and the coalescence of microscopic cavities leads to the initiation of macroscopic crack. The development of microscopic, mesoscopic and the macroscopic processes of fracture in materials together with the resulting deterioration in their mechanical properties is called damage. Continuum damage mechanics, in particular, aims at the analysis

of the damage development in mesoscopic and macroscopic fracture processes in the framework of continuum mechanics.

The seperation of atomic bonds is induced either by shear or tensile decohesion. However the separation of material at the microscopic level consists of four damage mechanisms namely Cleavage, Growth and Coalescence of Microvoids, Glide plane decohesion and Void Growth due to Grain-Boundary diffusion. The aspects of damage vary largely by difference in materials and loading conditions. The damage may be classified phenomenologically as follows

- Ductile Damage

- Brittle Damage

- Creep Damage

- Low Cycle Fatigue

- Very Low Cycle Fatigue

- High Cycle fatigue damage

- Very High Cycle fatigue damage

- Creep Damage

0.2.2   Representative Volume Element(RVE)

In order to discuss the effects of microscopic discontinuities in a material by means of CDM we must homogenize the mechanical effects of microstructure and represent them as a macroscopic continuous field in the material. For this purpose we take a small region of a mesoscale around the material point P(x) in a body B as showin in Fig. 2. We assume that the material with discontinuous structures in this region can be statistically homogeneous and the mechanical state of the material in this region can be represented by the statistical average of the mechanical variables in that region. This region is said to be the Representative Volume Element(RVE). For such RVE, the following two conditions must be satisfied:

- For the material in the RVE to be statistically homogeneous, the RVE should be large enough to contain a sufficient number of discontinuities

- In order to represent a non-uniform macroscopic mechanical field by means of a continuum, the size of RVE should be sufficiently small so that the variation of the macroscopic variable in it may be insignificantly small

The size of RVE depends on the microstructure of the relevant material and their typical sizes are as follows

- Metals and ceramics - $0.1mm^3$

- Polymer and composites - $1mm^3$

- Timber - $10mm^3$

- Concrete - $100mm^3$

0.2.3 Concept of Continuum damage mechanics (CDM)

The basic concept of CDM is that the microstructural defects in a material can be represented by a set of damage variables. Continuum damage mechanics first represent the damage state of a material in terms of properly defined damage variables and then describe the mechanical behaviour of the damaged material and then development of damage by use of these damage variables. The mechanical behaviour of a damaged material can be described using the notion of effective stress, together with hypothesis of mechanical equivalence between damaged and undamaged material. The concept of effective stress and mechanical equivalence will be discussed in the following sections.

Modelling by Effective Area Reduction

Let us consider a body B of Fig. (3) and take a representative volume element(RVE) at an arbitrary point $P(x)$ in B. If the total void area in dA is dA_D, the mechanical effect of dA will be decreased by dA_D. Then the area,

$$d\tilde{A} = dA - dA_D \tag{1}$$

may be interpreted as the area which carries the internal force and is called as *effective area*. Thus the damage variable D can be specified as

$$D = \frac{dA - d\tilde{A}}{dA} = \frac{dA_D}{dA} \tag{2}$$

where the damage variable D takes value between 0 and 1 ($0 \leq D \leq 1$). $D = 0$ representing initial undamaged state and $D = 1$ represents fully damaged state. Suppose a cylindrical bar of cross-sectional area dA is subject to a tensile load dF the actual load carrying area is $d\tilde{A}$ rather than dA. According to eqn (1) and (2) the effective area $d\tilde{A}$ is given by,

$$d\tilde{A} = (1 - D)dA \tag{3}$$

The decrease in load-carrying area increase the effect of stress σ induced by the external force dF. Due to eqn 3 the magnified stress $\tilde{\sigma}$ is given by,

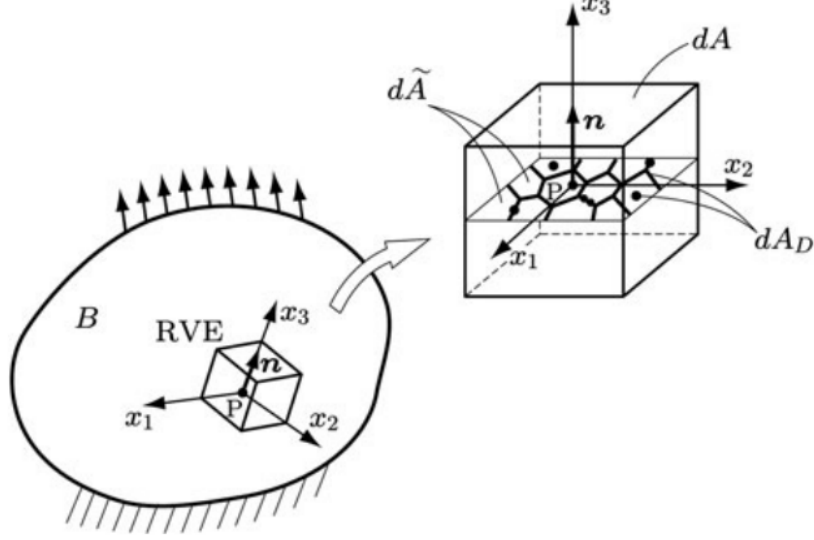$$\tilde{\sigma} = \frac{dF}{d\tilde{A}} = \frac{\sigma}{1 - D} \tag{4}$$

Figure 3: Effective area reduction due to microcracks

Since the stress $\tilde{\sigma}$ represents the effect of stress magnified by the net area reduction due to damage, it is called as *effective stress*. From eqn (3) and (4) we can postulate that the damaged cylindrical bar of Fig.(4b) with the cross-sectional area dA subject to force dF is mechanically equivalent to the fictious undamaged bar of Fig.(4c) which is subject to force dF , has the cross-sectional area $d\tilde{A}$ and hence stress has the stress $\tilde{\sigma}$

Modelling by variation of elastic modulus

Since the development of microcracks induces the reduction in stiffness of material, the damage state can be characterized by variation in elastic modulus. Let us consider the bar (b) and (c) of Fig. (4) are in damaged and fictitious undamaged state respectively. Then the elastic strain ϵ in the bar (c) caused by stress $\tilde{\sigma}$ should be equal to the ϵ of the bar (b) under stress σ; i.e.,

$$\tilde{\sigma} = E_0\epsilon, \;\; \sigma = E(D)\epsilon \tag{5}$$

$$\epsilon = \frac{\sigma}{E(D)} = \frac{\tilde{\sigma}}{E_0} \tag{6}$$

where E_0 and $E(D)$ denote young's modulus of the material in the initial undamaged state and that in damaged state after loading, respectively. Therefore, eqn. (6) defines another effective stress
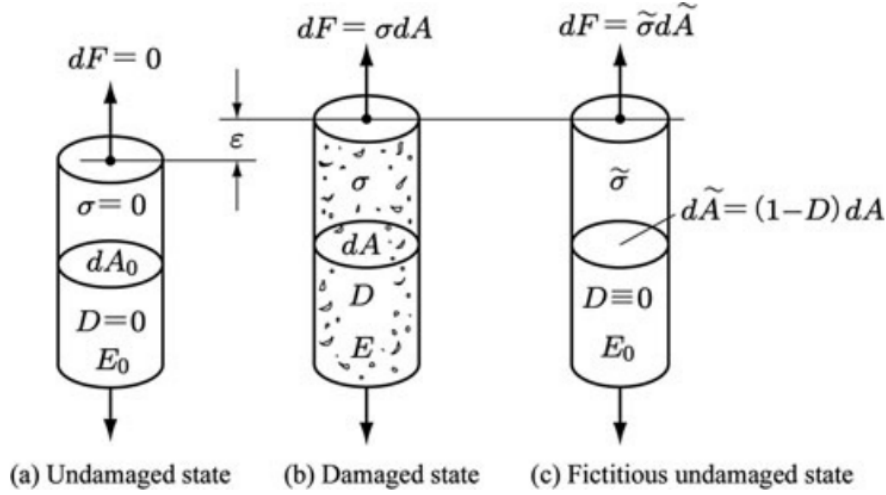
8

Figure 4: Damage of bar under tensile load

$$\epsilon = \frac{E_0}{E(D)}\sigma \tag{7}$$

By combining Eqn. (4) and (6) we get,

$$E(D) = (1 - D)E_0 \tag{8}$$

$$D = 1 - \frac{E(D)}{E_0} \tag{9}$$

Therefore, the damage variable D is characterized by the variation in Young's modulus $E(D)$. The modelling of damage by means of reduction in stiffness can be applied also the anisotropic damage of brittle materials like composite materials, concrete, rocks etc.,

0.2.4 Mechanical representation of three dimensional damage state

The deformation of a material basically depends on the direction of applied stress or strain and hence it is an anisotropic phenomenon. Therefore different theories have been developed for modelling 3-D anisotropic damage phenomenon. Some fundamental theories that describes 3-D damage state are given below

Scalar Damage Variable

In case of random or isotropic distribution of microcracks or voids , the damage state is usually considered as isotropic. the damage state in this case may be

represented by means of scalar damage variable D. When microvoids have oriented distribution the damage state is anisotropic and the scalar damage variable cannot be applied accurately. However, when void density is small the global mechanical properties can be approximated as nearly isotropic. Thus isotropic damage theory based on isotropic damage variable has been often applied to 3-D problems of creep, elastic-plastic, ductile and fatigue damage

Plural Scalar damage variables

A single scalar damage variable is often insufficient to describe the variation in mechanical properties of the damaged materials, even if the distribution of microcracks are isotropic. Plural scalar damage variables are often employed to characterize several different microscopic mechanisms of the relevant damage development.

Vector damage variable

The damage state can be specified by the decrease in load carrying effective area due to void development. Hence it is easy to postulate a vector damage variable. Kachanov (1974, 1986) tried to extend the definition of damage to anisotropic damage by noting a surface element in an arbitrary direction n, he proposed a vector damage variable $\omega = \omega_n n$, where ω_n is the effective area fraction.

Damage tensor of second order

In order to describe an anisotropic damage state, damage variable of second or higher order tensor is required. Eqn.(3) suggests that the damage state (1 - D) is specified by the transformation of the surface element dA of Fig. (4b) of the damage state into the corresponding surface element $d\tilde{A}$ in the fictitious undamaged state of Fig.(4c). In order to express damage as a second order tensor, we first consider an
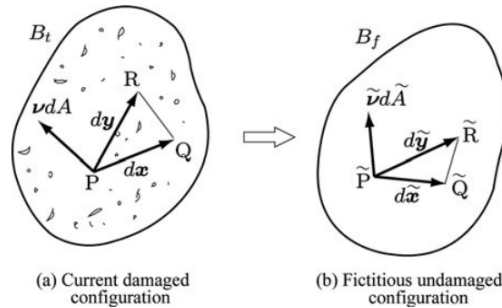

(a) Current damaged configuration

(b) Fictitious undamaged configuration

Figure 5: Surface element in RVE of a damaged material

arbitrary surface element PQR in RVE in the current damaged configuration B_t of

Fig.(5a) . The unit normal vector and area of PQR are denoted by ν and dA. We further postulate the fictitious undamaged configuration B_f of Fig.(5b) mechanically equivalent to B_t, and the surface element and its area vector are denoted by $\tilde{P}\tilde{Q}\tilde{R}$ and $\tilde{\nu}d\tilde{A}$ respectively. According to Eqn.(3) the damage variable of second-order tensor D should be defined by linear transformation from area vector νdA in B_t into $\tilde{\nu}d\tilde{A}$ in B_f, i.e.,

$$\tilde{\nu}d\tilde{A} = (I - D)\nu dA \tag{10}$$

where I is the second order identity tensor. Since the damage tensor D is symmetric, it can be expressed by its spectral decomposition

$$D = \sum_{i=1}^{3} D_i n_i \otimes D_i n_i \tag{11}$$

where D_i and n_i are the principal value and principal direction of D.

0.2.5 Effective Stress Tensors

The effective stresses are used to describe the mechanical behaviour of the damaged material. Some of the effective stresses postulated in damage mechanics are given below

Effective Stress Tensor for Isotropic Damage

If the damage state is isotropic then the effective stress tensor of three-dimensional state is given by

$$\tilde{\sigma} = (1 - D)^{-1} \sigma \tag{12}$$

where D is the scalar damage variable and σ is the Cauchy stress tensor. This effective stress simplifies damage theory and can be applied to number of damage problems like ductile damage. But this cannot be applied to damage of significant anisotropy, such as brittle damage due to microcrack distribution

Asymmetric Effective Stress Tensor for Anisotropic Damage

The increase in stress effect caused by the net area reduction in case of anisotropic damage is given by

$$\tilde{\sigma} = (I - D)^{-1} \sigma \tag{13}$$

where I and D are second order identity tensor and the second order damage tensor respectively. In the actual development of anisotropic damage, the stress induced in RVE of damage material is asymmetric. But asymmetric stress tensor makes the numerical analysis complicated and thus different methods of symmetrization has been proposed. Few of them are described as follows

Symmetrized Effective Stress Tensor for Anisotropic Damage 1 (Murakami and Ohno 1981)

A simple symmetrization procedure of Eq.(14), the symmetric part of the Cartesian decomposition of Eq.(14) gives,

$$\tilde{\sigma} = \frac{1}{2}[(I - D)^{-1}\,\sigma + \sigma(I - D)^{-1}]$$ (14)

Symmetrized Effective Stress Tensor for Anisotropic Damage 2 (Cordebois and Sidoroff 1982a, b)

Another form of symmetrization was proposed by Cordebois and Sidoroff:

$$\tilde{\sigma} = (I - D)^{-1/2}\sigma(I - D)^{-1/2}$$ (15)

where σ and D are co-axial. Moreover, unless the development of damage is large, the difference between these effective stresses are known to be insignificant.

0.2.6 Matrix Representation of Damage effect tensors

The general form of an effective stress tensor $\tilde{\sigma}$ is given by the damage effect tensor $\mathbb{M}$ and the corresponding Cauchy stress tensor σ, i.e.,

$$\tilde{\sigma} = \mathbb{M} : \sigma$$ (16)

It is convenient to express the tensors in the form of matrices and then execute the tensor operations as a matrix calculus.. To simplify this procedure, we take an orthonormal basis n_i with principal directions n_i of the second-order symmetric damage tensor D, and represent the the tensor in terms of their component to this basis. According to voigt notation, the second-order symmetric tensor σ and the related effective stress $\tilde{\sigma}$ are expressed by column vector of six dimension:

$$[\sigma_P] \equiv [\sigma_{11} \ \ \sigma_{22} \ \ \sigma_{33} \ \ \sigma_{12} \ \ \sigma_{13} \ \ \sigma_{23}]^T$$ (17)

$$[\tilde{\sigma_P}] \equiv [\tilde{\sigma_{11}} \ \ \tilde{\sigma_{22}} \ \ \tilde{\sigma_{33}} \ \ \tilde{\sigma_{12}} \ \ \tilde{\sigma_{13}} \ \ \tilde{\sigma_{23}}]^T$$ (18)

The damage effect tensor $\mathbb{M}$ can be represented as symmetric matrix. By representing first two indices ij and the succeeding two indices kl of the tensor by p and q ($p, q = $ 1,2,...,6), respectively, the components of $\mathbb{M}$ are expressed by a six by six matrix

$$
[\mathbb{M}_{pq}] \equiv
\begin{bmatrix}
M_{1111} & M_{1122} & M_{1133} & M_{1123} & M_{1131} & M_{1112} \\[1em]
M_{2211} & M_{2222} & M_{2233} & M_{2223} & M_{2231} & M_{2212} \\[1em]
M_{3311} & M_{3322} & M_{3333} & M_{3323} & M_{3331} & M_{3312} \\[1em]
M_{2311} & M_{2322} & M_{2333} & M_{2323} & M_{2331} & M_{2312} \\[1em]
M_{3111} & M_{3122} & M_{3133} & M_{3123} & M_{3131} & M_{3112} \\[1em]
M_{1211} & M_{1222} & M_{1233} & M_{1223} & M_{1231} & M_{1212}
\end{bmatrix}
$$

By means of the matrix representation, we have the matrix form

$$
[\tilde{\sigma}_P] \equiv [\mathbb{M}_{pq}] \; : [\sigma_P] \tag{19}
$$

Matrix representation of the damage effect tensor of Eq.(19) is shown below

$$
[\mathbb{M}_{pq}] \equiv
\begin{bmatrix}
\frac{1}{\omega_{11}} & 0 & 0 & 0 & 0 & 0 \\[1em]
0 & \frac{1}{\omega_{22}} & 0 & 0 & 0 & 0 \\[1em]
0 & 0 & \frac{1}{\omega_{33}} & 0 & 0 & 0 \\[1em]
0 & 0 & 0 & \frac{1}{\omega_{12}} & 0 & 0 \\[1em]
0 & 0 & 0 & 0 & \frac{1}{\omega_{23}} & 0 \\[1em]
0 & 0 & 0 & 0 & 0 & \frac{1}{\omega_{13}}
\end{bmatrix}
$$

where

$$
\omega_{11} = (1 - d_1) \quad \omega_{22} = (1 - d_2) \quad \omega_{33} = (1 - d_3)
$$

$$
\omega_{12} = \sqrt{(1 - d_1)(1 - d_2)} \quad \omega_{23} = \sqrt{(1 - d_2)(1 - d_3)} \quad \omega_{13} = \sqrt{(1 - d_1)(1 - d_3)}
$$

0.2.7 Hypothesis of Strain Equivalence

The inelastic constitutive equation of a damaged material is given by the corresponding constitutive equation for an undamaged material by replacing the stress tensor σ in the equation with the corresponding effective stress tensor $\tilde{\sigma}$. In Fig. the effect of stress σ acting on RVE in the current damaged configuration B_t is equivalent to that of the stress $\tilde{\sigma}$ in the fictitious undamaged configuration. Therefore the deformation of the damaged material subject to stress σ should be equal to that of the fictitious undamaged material subject to stress $\tilde{\sigma}$. Suppose the constitutive equation of an undamaged inelastic material is given by

$$\epsilon = F_0(\sigma, \alpha) \tag{20}$$

or

$$\dot{\epsilon} = F_0(\sigma, \alpha) \tag{21}$$

where α is an internal variable representing the internal change other than damage. and $(\dot{})$ denotes the material time derivative Then according to hypothesis of strain
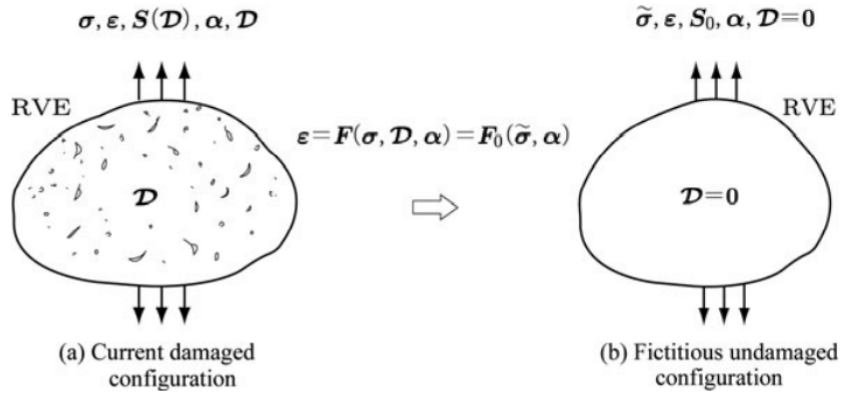

Figure 6: Hypothesis of strain equivalence

equivalence, the inelastic constitutive equation of the damaged material represented by a damage variable D should be given by replacing σ of Eq.(25) with the effective stress $\tilde{\sigma}$ i.e.,

$$\epsilon = F(\sigma, D, \alpha) = F_0(\tilde{\sigma}, \alpha) \tag{22}$$

or

$$\dot{\epsilon} = F(\sigma, D, \alpha) = F_0(\tilde{\sigma}, \alpha) \tag{23}$$

In case of elastic deformation, constitutive equations for an undamaged and damaged material is given by

$$\epsilon = \mathbb{S}_0 : \sigma, \tag{24}$$

$$\epsilon = \mathbb{S}(D) : \sigma, \tag{25}$$

where $\mathbb{S}_0$ and $\mathbb{S}(D)$ are fourth-order elastic compliance tensors of the materials. Therefore, according to the hypothesis of strain equivalence the elastic constitutive equation of the damaged material and the compliance tensor is given by

$$\epsilon = \mathbb{S}_0 : \tilde{\sigma} = [\mathbb{S}_0 : \mathbb{M}(D)] : \sigma = \mathbb{S}(D) : \sigma \tag{26}$$

$$\mathbb{S}(D) = \mathbb{S}_0 : \mathbb{M}(D) \tag{27}$$

where $\mathbb{M}(D)$ is the damage effect tensor which is given by

$$\mathbb{M}(D) = \mathbb{S}_0^{-1} : \mathbb{S}(D) \tag{28}$$

The resulting compliance tensor of Eq.(27) has inconvenience of its asymmetry which can resolved by taking another variable D^* besides D.

$$\mathbb{S}^*(D) = \frac{1}{2}[\mathbb{S}_0 : \mathbb{M}(D^*) + \mathbb{M}^T(D^*) : \mathbb{S}_0] \tag{29}$$

and

$$\mathbb{M}(D^*) = \frac{1}{2}[\mathbb{M}(D^*) + \mathbb{S}_0^{-1} : \mathbb{M}^T(D^*) : \mathbb{S}_0] \tag{30}$$

0.2.8   Hypothesis of strain energy equivalence

Let us consider an elastic-plastic material, and represent the internal change due to plastic deformation by an internal state variable α. The complementary strain energy functions of the material at undamaged and damaged state are given, respectively as follows

$$V_0(\sigma, \alpha) = \frac{1}{2}\sigma : \mathbb{S}_0 : \sigma \ - \ \phi(\alpha) \tag{31}$$

$$V(\sigma, D, \alpha) = \frac{1}{2}\sigma : \mathbb{S}(D) : \sigma \ - \ \phi(\alpha) \tag{32}$$

Thus the constitutive equation for the undamaged and damaged material

$$\epsilon = \frac{\partial V_0}{\partial \sigma} = \mathbb{S}_0 : \sigma \tag{33}$$

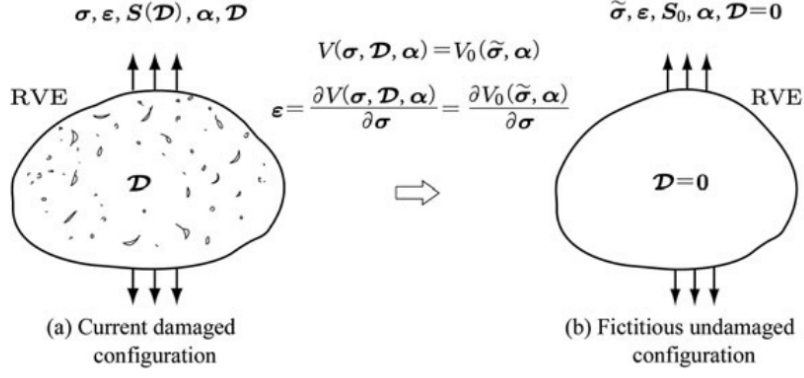$$\epsilon = \frac{\partial V}{\partial \sigma} = \mathbb{S}(D) : \sigma \tag{34}$$

$\sigma, \varepsilon, \mathbb{S}(\boldsymbol{D}), \boldsymbol{\alpha}, \boldsymbol{D}$ $\widetilde{\sigma}, \varepsilon, \mathbb{S}_0, \boldsymbol{\alpha}, \boldsymbol{D}{=}0$

$V(\sigma, \boldsymbol{D}, \boldsymbol{\alpha}) = V_0(\widetilde{\sigma}, \boldsymbol{\alpha})$

$\varepsilon = \dfrac{\partial V(\sigma, \boldsymbol{D}, \boldsymbol{\alpha})}{\partial \sigma} = \dfrac{\partial V_0(\widetilde{\sigma}, \boldsymbol{\alpha})}{\partial \sigma}$

RVE   RVE

$\boldsymbol{D}$ $\boldsymbol{D}{=}0$

(a) Current damaged   (b) Fictitious undamaged
configuration   configuration

Figure 7: Hypothesis of strain energy equivalence

Suppose a damaged material of Fig.(7)a subject to stress σ, and represent the damage and internal state due to inelastic deformation by D and α, respectively. Then the strain energy function $V(\sigma, D, \alpha)$ of the damaged material is given by replacing σ in the corresponding function $V_0(\sigma, \alpha)$ of the undamaged material of Fig.(7)b with effective stress $\tilde{\sigma}$

$$V(\sigma, D, \alpha) = V_0(\tilde{\sigma}, \alpha)$$

By the use of this hypothesis, the elastic strain of Eq.(34) leads to

$$\epsilon = \frac{\partial V(\sigma, D, \alpha)}{\partial \sigma} = \mathbb{S}(D) : \sigma$$

$$= \frac{\partial V_0(\tilde{\sigma}, \alpha)}{\partial \sigma} = \frac{\partial}{\partial \sigma}(\frac{1}{2}\tilde{\sigma} : \mathbb{S}_0 : \tilde{\sigma})$$

$$= \frac{1}{2}\frac{\partial}{\partial \sigma}[(\mathbb{M}(D) : \sigma) : \mathbb{S}_0 : (\mathbb{M}(D) : \sigma)]$$

$$= [\mathbb{M}^T(D) : \mathbb{S}_0 : \mathbb{M}(D)] \tag{35}$$

From Eq.(35), the elastic compliance tensor of the damaged material is given as follows

$$\mathbb{S}(D) = \mathbb{M}^T(D) : \mathbb{S}_0 : \mathbb{M}(D) \tag{36}$$

16

In relation to the effective stress tensor $\tilde{\sigma}$ of Eqn.(16) we may define a new effective strain tensor

$$\tilde{\epsilon} \;=\; \mathbb{M}^{-T}(D) : \epsilon \tag{37}$$

Then the complementary strain energy function and the elastic constitutive equation can be written also in the form

$$V = \frac{1}{2}\sigma : \epsilon \;-\; \phi(\alpha) = \frac{1}{2}\tilde{\sigma} : \tilde{\epsilon} \;-\; \phi(\alpha) \tag{38}$$

$$\tilde{\epsilon} \;=\; \mathbb{S}_0 : \tilde{\sigma} \tag{39}$$

0.2.9 Elastic Constitutive equation and Elastic modulus tensor of orthotropic material

Orthotropic materials are materials which exhibit different material properties along three mutually-orthogonal axis. They are a special form of anisotropic materials, because their properties change when measured from different directions. Some examples of orthotropic materials are wood, composite materials etc., Orthotropic materials require 9 independent variables in order to express their constitutive matrix. The 9 elastic constants are three Young's moduli E_x, E_y, E_z, the three Poisson's ratios $\nu_{xy}, \nu_{yz}, \nu_{zx}$, and three shear moduli G_{xy}, G_{yz}, G_{zx}. The elastic stiffness matrix of orthotropic material has the form,

$$\sigma = \mathbb{C}_0 : \epsilon \, or \quad \sigma_{ij} = C^0_{ijkl}\epsilon_{kl}, \tag{40}$$

$$[C^0_{pq}] = \begin{bmatrix} \frac{1-\nu_{yz}\nu_{zy}}{E_y E_z \Delta} & \frac{\nu_{xy}+\nu_{xz}\nu_{zy}}{E_y E_z \Delta} & \frac{\nu_{xz}+\nu_{xy}\nu_{yz}}{E_y E_z \Delta} & 0 & 0 & 0 \\[2ex] \frac{\nu_{yx}+\nu_{yz}\nu_{zx}}{E_x E_z \Delta} & \frac{1-\nu_{xz}\nu_{zx}}{E_1 E_z \Delta} & \frac{\nu_{yz}+\nu_{yx}\nu_{xz}}{E_1 E_z \Delta} & 0 & 0 & 0 \\[2ex] \frac{\nu_{zx}+\nu_{yx}\nu_{zy}}{E_x E_y \Delta} & \frac{\nu_{zy}+\nu_{xy}\nu_{zx}}{E_x E_y \Delta} & \frac{1-\nu_{xy}\nu_{yx}}{E_x E_y \Delta} & 0 & 0 & 0 \\[2ex] 0 & \nu & \nu & G_{xy} & 0 & 0 \\[2ex] 0 & \nu & \nu & 0 & G_{yz} & 0 \\[2ex] 0 & \nu & \nu & 0 & 0 & G_{zx} \end{bmatrix}$$

where

$$\Delta = (1 - \nu_{xy}\nu_{yx} - \nu_{yz}\nu_{zy} - \nu_{zx}\nu_{xz} - 2\nu_{xy}\nu_{yz}\nu_{zx})/E_x E_y E_z$$

and $\frac{\nu_{xy}}{E_y} = \frac{\nu_{yx}}{E_x}, \frac{\nu_{yz}}{E_z} = \frac{\nu_{zy}}{E_y}, \frac{\nu_{xz}}{E_z} = \frac{\nu_{zx}}{E_x}$

0.3   Working environment

The material models necessary for simulating progressive damage models must be programmed first using a programming language, compiled and then can be tested in a commercial FEM software. The programming language of choice for most commercial FEM software is FORTRAN because they are simple and fast. In order to program the material model, an integrated development environment (IDE) and a compiler which is compatible with the version of the FEM software is required. In this chapter the tools required for creating material model and how to use them in order to test the models is described in detail.

0.3.1   Software tools required

- **OCTAVE**

    Octave is an open source version of programming language software MATLAB. Initially, the user material subroutines are developed on Octave and tested using simple tests like uniaxial tension with the help of constitutive driver routines

- **Visual studio**

    Visual studio is the IDE used for programming and debugging user material subroutines using FORTRAN programming language.
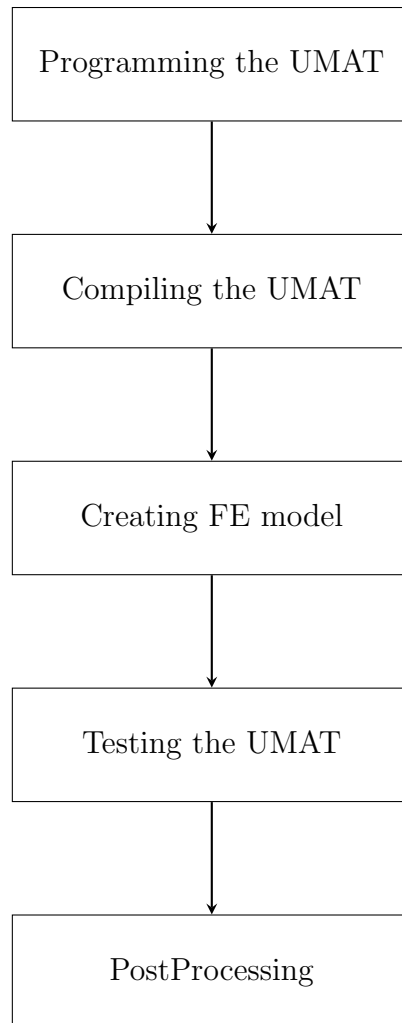
- **Intel parallel studio**

    The compiler available in Intel parallel studio is used for compiling the material subroutines before testing them in an FEM software

- **ANSYS**

    ANSYS is the commercial FEM software chosen for creating specimens and analyzing how the material models behave in different test conditions

The following sections provide the reader a detailed description starting from how to develop the user defined material subroutine to how to implement and analyse the

results in the ANSYS environment. The flowchart below shows the steps involved in the whole process

```
┌─────────────────────────────┐
│     Programming the UMAT     │
└─────────────────────────────┘
               │
               ▼
┌─────────────────────────────┐
│      Compiling the UMAT      │
└─────────────────────────────┘
               │
               ▼
┌─────────────────────────────┐
│       Creating FE model      │
└─────────────────────────────┘
               │
               ▼
┌─────────────────────────────┐
│       Testing the UMAT       │
└─────────────────────────────┘
               │
               ▼
┌─────────────────────────────┐
│        PostProcessing        │
└─────────────────────────────┘
```

0.3.2   Programming the UMAT

The user material subroutine is an ANSYS programmable feature which allows user to write their own material constitutive equations with in a newly developed general material framework. The subroutine is called at all material integration points of the element during solution phase. ANSYS uses FORTRAN as the programming language for creating user programmable features. Therefore Visual Studio is the IDE used for developing these FORTRAN subroutines.

ANSYS demands the necessary variables declared in certain way so that the USERMAT developed can work compatibly with ANSYS when it is called at each integration points. The guidelines for declaring input and output arguments can be found on ANSYS' usermat guide. The following image shows the user subroutine in-

terface with the set of possible input arguments that can accessed by USERMAT from
ANSYS

```
subroutine usermat(
&                matId, elemId,kDomIntPt, kLayer, kSectPt,
&                ldstep,isubst,keycut,
&                nDirect,nShear,ncomp,nStatev,nProp,
&                Time,dTime,Temp,dTemp,
&                stress,statev,dsdePl,sedEl,sedPl,epseq,
&                Strain,dStrain, epsPl, prop, coords,
&                tsstif, epsZZ,
&                var1, var2, var3, var4, var5,
&                var6, var7, var8)

 INTEGER
&                matId, elemId,
&                kDomIntPt, kLayer, kSectPt,
&                ldstep,isubst,keycut,
&                nDirect,nShear,ncomp,nStatev,nProp
 DOUBLE PRECISION
&                Time,    dTime,    Temp,    dTemp,
&                sedEl,   sedPl,   epseq,   epsZZ
 DOUBLE PRECISION
&                stress  (ncomp  ), statev  (nStatev),
&                dsdePl  (ncomp,ncomp),
&                Strain  (ncomp  ), dStrain (ncomp  ),
&                epsPl   (ncomp  ), prop     (nProp  ),
&                coords  (3),          rotateM (3,3),
&                defGrad_t(3,3),     defGrad(3,3),
&                tsstif  (2)
```

Figure 8: Usermat Interface

For every Newton raphson iteration, the USERMAT is called at every material
integration point and the ANSYS passes in strains, stresses and state variables at the
beginning of the time increment and the current strain increment. The USERMAT
then has to compute and update the necessary output arguments like stresses and
state variables at the end of the increment and the material tangent stiffness matrix
$\frac{\partial \sigma}{\partial \epsilon}$.

0.3.3 Compiling UMAT

The user programmable subroutines must be compiled before testing them in
ANSYS environment. The process of compilation first checks for errors in the source
and then converts them into ANSYS executable files (.dll files) which then can be used
by ANSYS. The compiler present in Intel parallel studio is used for this purpose. The

step by step process of compiling the UMAT is given below

- Create an empty directory and copy the usermat file that you want to compile (.f files) into the empty directory.

- Change the name of your usermat file to *usermat*

- Go to "Control Panel>Search System>Edit the system environment variables>Environment variables" and click New in the user variables for your PC which opens a window

- In that window, type ANS_USER_PATH for variable name and for variable value, copy and paste the path to your working directory and click Ok

- Go to folder "C:\ Program Files\ ANSYS Inc\ v181\ ansys\ custom\ user\ win64" and copy the ANSUSERSHARED.bat file and paste it in the working directory

- Open command prompt and navigate to the working directory

- Type ANSUSERSHARED.bat and press enter. This opens the Intel compiler and asks for user-programmable feature source file name

- Type *usermat* without extension and press Enter.

- If there is no error in the usermat file the compiler will show the message "usermatLib.dll has been successfully build."

- In order for the ANSYS to access these .dll files, open ANSYS Mechanical APDL product launcher and in the file management section browse to the current working directory

- Click run and in the Mechanical APDL output window you shoud see the message "Note - This ANSYS version was linked by Licensee". This indicates that you are using the shared library with the USERMAT

0.3.4 Creating FE model

The preprocessor section of the ANSYS mechanical APDL is used to create and mesh the FE model. The ANSYS user programmable feature can be used with 18x family elements, which include LINK180, PLANE 182, PLANE 183, SOLID 185, SOLID 186. The type of element required for creating FE model based on the problem can be chosen from the element type menu in preprocessor section. Once the element type is chosen the material model and the material properties can be entered in the

Material props section. The *Modelling* section can be utilised to create the geometry required for testing the subroutines and then can be meshed using the *Meshing* option.

In order to use the FE model again and again to test different material models with different material properties the FE model can be saved in the form of an APDL script. An APDL script is a simple text file which contains the command required to create and solve and FE model. A simple way to create an APDL script for an FE model is to copy the log of commands which were automatically created in the log file during the creation of your model and pasting it a new text file. This log file can be accessed by going to *List > Files > Logfile*. The created APDL script can then be accessed by going to *File > Read input from* and navigate and select your file.

0.3.5   Testing UMAT

To use the user material option, the TB,USER command must be included in the APDL script so that the user material can be defined. The table command for USER material option is

TB,USER,matId,NTEMPS,NPTS

matId - material reference number

NTEMPS - Number of temperature points

NPTS - Number of material constants at a given temperature

If state variables are used in the subroutine, the number of state variables need to be defined in the APDL script by the command TB,STATE

TB,STATE,matId,,NPTS

matId - material reference number

NPTS - Number of state variables to be used in USERMAT

A simple example for defining user material and two state variables is given int the Fig.(9) below Before defining boundary conditions (BCs) the entities required for

solving the FE model such as time at the end of load step, number of steps, the results to be stored etc., must be defined. This can be done using *Sol'n Controls* option in

```
!*
YOUNG = 210e3
POISSON = 0.33
T1 = 1

TB,USER,1,1,2,
TBTEMP,T1
TBDATA,,YOUNG,POISSON
TB,STATE,1,,2
```

Figure 9: Table (TB) commands

the solution menu. Once the BCs are defined the model can be solved by giving the command $SOLVE$.

0.3.6 PostProcessing

Once the FE model has finished solving, the results then can be analyzed using the 'General Postprocessor' option. The nodal and elemental solution for components like stress, strain, displacement etc., can be plotted using the 'contour plot' option which can be found on Plot results. By default this option plots the results at last sub step, so to plot the solution at the sub step of your choice one must navigate to $Read\ results > By\ pick$ and select the substep to be plotted. Then the results of that substep can be plotted using 'contour plot' option mentioned before. Since the posprocessor of ANSYS doesnot have GUI option for plotting state variables the following command must be given: $plnsol, svar, n$ where n is the number of the state variable to be plotted.

The time history of a certain variable such stress,reaction force, strain etc., at a node or an element can be plotted using $TimeHist\ Postpro$ option. On clicking the $TimeHist\ Postpro$ option a $Variable\ List$ window opens up. In order to add the variables to plot, click the green add symbol on the top-left corner which opens a window with the list of variables that can be added to the $Variable\ List$ window. Once the variables has been added the variables can be plotted against each other or against time. Fig.(10) shows the $Variable\ List$ window with X-component of force and displacement of node 3 selected and plotted against each other. The time history results of each variable at node or an element can also be saved as text file using $List\ Data$ option in the $Variable\ List$ window.
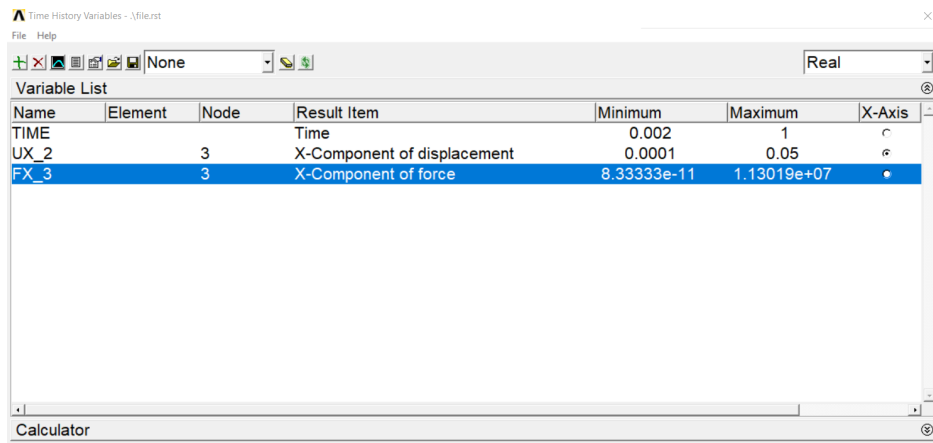
Figure 10: Time history post processor window

0.4 Progressive Failure analysis of Orthotropic composite materials

0.4.1 Fibre-reinforced Composites

Fibre reinforced plastic composites is a term for large family of materials ranging from short fibre reinforced polyesters to unidirectional graphite fibre epoxies. Fibre reinforced composites consists of three components 1) the fibres as the discontinuous or dispersed phase 2) the matrix as the continuous phase and 3) the fine inter-phase region also known as the interface. The different combination of fibre and matrix material lead to different material properties and also the manifestation of the fibres and the manufacturing techniques. The first fibres used in fibre reinforced plastics are made of glass. Although the virgin strength of the glass is high, the actual strength is limited by the microscopic defects on the surface of the fibre. The graphite fibres are anisotropic due to their laminar structure. Graphite fibres maintain their strength even at high temperatures. Two types of plastics are commonly used as matrix materials, namely unsaturated polyesters and epoxies. The use of unsaturated polyesters is restricted to temperatures upto 100C. The main advantage of this material is the high amount of shrinkage at hardening , which causes high internal stress and decrease the strength of the material. The characteristics of epoxy are better than polyester resins. The material can withstand temperatures upto 250C and shrinks only 2% at hardening. But epoxy resins are high in price compared to the polyesters.

0.4.2 Mechanisms of damage and failure in fibre reinforced composites

The failure in fibre reinforced composites happens mainly due to matrix cracking or fibre failure. Therefore the failure can be divided mainly two types namely 1) Longitudinal failure and 2) Transverse failure. The mechanism of both failure mechanisms, its causes and its effects on material behaviour are discussed in detail below

Longitudinal failure

In fibre-reinforced plastics, the largest portion of the load is resisted by fibres. When the fibres fail, the load must redistribute to other areas of the structure, and may

cause structural collapse. In composites where strain to failure for resin matrix is higher than one of the reinforcing fibre, longitudinal failures start by isolated fibre fractures in weak zones. This kind of localized fractures increase the normal and interfacial shear stress in fibres and promote matrix cracking, fibre matrix debonding, conical shear failures etc., When the load is further increased it may lead to final collapse. Longitudinal tensile failure occurs in both constituents, and a fracture occurs along a plane whose normal is parallel to the fibre direction. A simple maximum stress or maximum strain can usually provide an accurate measure of longitudinal tensile failure. Longitudinal compressive failure occurs from the collapse of the fibres as a result of shear kinking and damage of the supporting matrix. Fibre misalignment causes shear stress between fibres that rotate fibres, which increases shear stress further and leads to instability.

Transverse failure

Transverse failure happens due to matrix cracking and fibre-matrix debonding. Under the presence of in-plane shear stress and transverse tensile stress, the combined effects of defects such as resin rich regins, fibre-resin debonds, and resin voids, trigger a transverse crack that extends through the thickness. The transverse cracks are formed at fibre-resin interface without affecting the fibres. When and unidirectional fibre composite is loaded in shear, a non-linear shear stress-strain behaviour is observed before the material fails by through thickness matrix cracking. This non-linear behaviour is due to the visco-plastic behaviour of the matrix, and from the nucleation of microvoids.
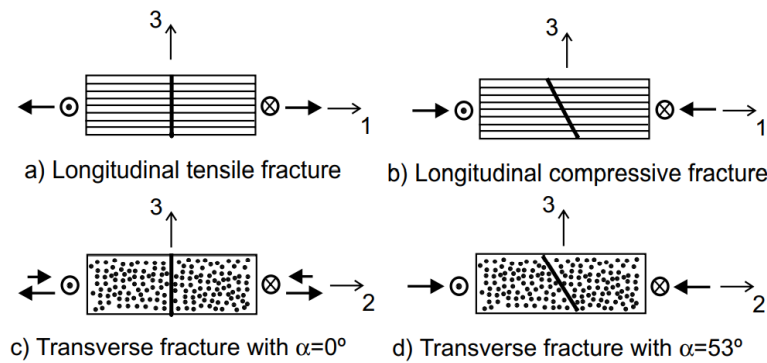
Figure 11: Fracture planes in FRP material

Experimental results have shown that moderate compression has beneficial effects on the strength of the material (Soden et al., 1998), when the transverse compressive

stress value is smaller compared to the in-plane shear stress, the fracture plane is perpendicular to the mid-plane of the ply. Increasing the compressive stress changes angle of the fracture plane. For glass-epoxy and carbon-epoxy composites when loaded in pure tranverse compression, the fracture plane is at an angle of 53° ± 3° with respect to thickness direction. Therefore, the matrix cracking does not occur in the plane of maximum transverse shear stress (45°).

0.4.3   Damage initiation criteria

Damage initiation criteria refers to the onset of damage at a material point. Since the properties of the orthotropic materials change in mutually perpendicular direction three failure mode index, F_f, F_m, F_z, are used for failure modes in three principal material directions. Since the failure due to tension and compression in each direction cannot happen at same integration point and at the same time, the failure mode index must be calculated based on whether the material direction is under tension or compression. Both strain and stress based damage initiation criteria can be employed based on the application. Some of the damage initiation criteria are given as follows

Maximum strain criteria

The maximum strain criterion is a simple criterion which checks whether the strain in the given material direction exceeds the failure strain or not. The maximum strain criterion for each material direction is given below

Damage direction	Tension	Compression
Fibre direction 1 (F_f)	$\dfrac{\epsilon_1}{\epsilon_{t1}} \leq 1$	$\dfrac{\epsilon_1}{\epsilon_{c1}} \leq 1$
Matrix direction 2 (F_m)	$\dfrac{\epsilon_2}{\epsilon_{t2}} \leq 1$	$\dfrac{\epsilon_2}{\epsilon_{c2}} \leq 1$
Matrix direction 3 (F_z)	$\dfrac{\epsilon_3}{\epsilon_{t3}} \leq 1$	$\dfrac{\epsilon_2}{\epsilon_{c3}} \leq 1$

Table 1: Maximum strain criterion

where ϵ_{ti} and ϵ_{ci} are failure strains in tension and compression respectively, in each

material direction.

Maximum stress criteria

Since the load-carrying area decreases due to increase in damage, the effective of stress gets magnified in the damaged material. Therefore, in case of maximum stress criteria normal stress components of the effective stress($\tilde{\sigma}$) are checked against the failure strength in each principal material direction. The effective stress can computed using the Eqn.(16). The maximum stress criteria for each material direction is given in the table below

Damage direction	Tension	Compression
Longitudinal direction 1 (F_f)	$\dfrac{\tilde{\sigma}_{11}}{X_T} \leq 1$	$\dfrac{\tilde{\sigma}_{11}}{-X_C} \leq 1$
Transverse direction 2 (F_m)	$\dfrac{\tilde{\sigma}_{22}}{Y_T} \leq 1$	$\dfrac{\tilde{\sigma}_{22}}{-Y_C} \leq 1$
Transverse direction 3 (F_z)	$\dfrac{\tilde{\sigma}_{33}}{Z_T} \leq 1$	$\dfrac{\tilde{\sigma}_{33}}{-Z_C} \leq 1$

Table 2: Maximum stress criterion

where X_T, Y_T and Z_T are failure strength in tension and X_C, Y_C and Z_C are failure strength in compression in each principal material direction respectively.

3D Hashin's quadratic strain criteria

Hashin's quadratic strain criteria includes shear strain components in addition to the normal strain components. The criteria for each material direction is given below

i) Longitudinal direction 1 ,

$$
F_f^2 = \begin{cases} \left(\dfrac{\epsilon_{11}}{\epsilon_{11}^{f,t}}\right)^2 + \left(\dfrac{\epsilon_{12}}{\epsilon_{12}^{f}}\right)^2 + \left(\dfrac{\epsilon_{13}}{\epsilon_{13}^{f}}\right)^2 \geq 1 & (\epsilon_{11} > 0) \\[3mm] \left(\dfrac{\epsilon_{11}}{\epsilon_{11}^{f,c}}\right)^2 \geq 1 & (\epsilon_{11} < 0) \end{cases}
\tag{41}
$$

ii) Transverse direction 2,

$$
F_m^2 = \begin{cases} \dfrac{(\epsilon_{22}+\epsilon_{33})^2}{\epsilon_{22}^{f,t}\epsilon_{33}^{f,t}} - \dfrac{\epsilon_{22}\epsilon_{33}}{(\epsilon_{23}^{f})^2} + \left(\dfrac{\epsilon_{12}}{\epsilon_{12}^{f}}\right)^2 + \left(\dfrac{\epsilon_{13}}{\epsilon_{13}^{f}}\right)^2 + \left(\dfrac{\epsilon_{23}}{\epsilon_{23}^{f}}\right)^2 \geq 1 & (\epsilon_{22} > 0) \\[3mm] \dfrac{(\epsilon_{22}+\epsilon_{33})^2}{\epsilon_{22}^{f,c}\epsilon_{33}^{f,c}} + \dfrac{\epsilon_{22}+\epsilon_{33}}{\epsilon_{22}^{f,c}}\left(\dfrac{\epsilon_{22}^{f,c}}{2\epsilon_{12}^{f}} - 1\right) - \dfrac{\epsilon_{22}\epsilon_{33}}{(\epsilon_{23}^{f})^2} + \left(\dfrac{\epsilon_{12}}{\epsilon_{12}^{f}}\right)^2 & (\epsilon_{22} > 0) \\[3mm] \qquad\qquad\qquad\qquad\qquad + \left(\dfrac{\epsilon_{13}}{\epsilon_{13}^{f}}\right)^2 + \left(\dfrac{\epsilon_{23}}{\epsilon_{23}^{f}}\right)^2 \geq 1 \end{cases}
\tag{42}
$$

iii) Transverse direction 3,

$$
F_z^2 = \begin{cases} \left(\dfrac{\epsilon_{33}}{\epsilon_{33}^{f,t}}\right)^2 + \left(\dfrac{\epsilon_{13}}{\epsilon_{13}^{f}}\right)^2 + \left(\dfrac{\epsilon_{23}}{\epsilon_{23}^{f}}\right)^2 \geq 1 & (\epsilon_{33} > 0) \\[3mm] \left(\dfrac{\epsilon_{33}}{\epsilon_{33}^{f,c}}\right)^2 + \left(\dfrac{\epsilon_{13}}{\epsilon_{13}^{f}}\right)^2 + \left(\dfrac{\epsilon_{23}}{\epsilon_{23}^{f}}\right)^2 \geq 1 & (\epsilon_{33} > 0) \end{cases}
\tag{43}
$$

in which $\epsilon_{ii}^{f,t} = \dfrac{\sigma_i^{f,t}}{C_{ii}}$, $\epsilon_{ii}^{f,c} = \dfrac{\sigma_i^{f,c}}{C_{ii}}$ $(i = 1, 2, 3)$, $\epsilon_{12}^{f} = \dfrac{\sigma_{12}^{f}}{C_{44}}$, $\epsilon_{13}^{f} = \dfrac{\sigma_{13}^{f}}{C_{55}}$, $\epsilon_{23}^{f} = \dfrac{\sigma_{23}^{f}}{C_{66}}$

3D Hashin's stress criteria

Hashin's stress criteria for each principal material direction is given as follows

i) Longitudinal direction 1,

$$
F_f^2 = \begin{cases} \left(\frac{\tilde{\sigma}_{11}}{X_T}\right)^2 + \left(\frac{\tilde{\sigma}_{12}}{S_{12}}\right)^2 + \left(\frac{\tilde{\sigma}_{13}}{S_{13}}\right)^2 \geq 1 & (\tilde{\sigma}_{11} > 0) \\[4mm] \left(\frac{\tilde{\sigma}_{11}}{X_C}\right)^2 \geq 1 & (\tilde{\sigma}_{11} < 0) \end{cases}
\tag{44}
$$

ii) Transverse direction 2,

$$
F_m^2 = \begin{cases} \left(\frac{\tilde{\sigma}_{22}}{Y_T}\right)^2 + \left(\frac{\tilde{\sigma}_{12}}{S_{12}}\right)^2 + \left(\frac{\tilde{\sigma}_{23}}{S_{23}}\right)^2 \geq 1 & (\tilde{\sigma}_{22} > 0) \\[4mm] \left(\frac{\tilde{\sigma}_{22}}{Y_C}\right)^2 + \left(\frac{\tilde{\sigma}_{12}}{S_{12}}\right)^2 + \left(\frac{\tilde{\sigma}_{23}}{S_{23}}\right)^2 \geq 1 & (\tilde{\sigma}_{22} < 0) \end{cases}
\tag{45}
$$

iii) Transverse direction 3,

$$
F_z^2 = \begin{cases} \left(\frac{\tilde{\sigma}_{33}}{Y_T}\right)^2 + \left(\frac{\tilde{\sigma}_{13}}{S_{13}}\right)^2 + \left(\frac{\tilde{\sigma}_{23}}{S_{23}}\right)^2 \geq 1 & (\tilde{\sigma}_{33} > 0) \\[4mm] \left(\frac{\tilde{\sigma}_{33}}{Y_C}\right)^2 + \left(\frac{\tilde{\sigma}_{13}}{S_{13}}\right)^2 + \left(\frac{\tilde{\sigma}_{23}}{S_{23}}\right)^2 \geq 1 & (\tilde{\sigma}_{33} < 0) \end{cases}
\tag{46}
$$

where X_T, Y_T and Z_T are failure strength in tension and X_C, Y_C and Z_C are failure strength in compression in each principal material direction respectively. S_{12}, S_{23}, and S_{13} are shear strengths.

Modified Hashin's failure criterion

Modified Hashin's failure criterion for plane stress condition is given below

i) Longitudinal direction 1,

$$
F_f = \begin{cases} \left[\left(\frac{\tilde{\sigma}_{11}}{X_T}\right)^2 + \alpha.\left(\frac{\tilde{\sigma}_{12}}{S}\right)^2\right]^{\frac{1}{2}} \geq 1 & (\tilde{\sigma}_{11} > 0) \\[4mm] \left[\left(\frac{\tilde{\sigma}_{11}}{X_C}\right)^2 + \alpha.\left(\frac{\tilde{\sigma}_{12}}{S}\right)^2\right]^{\frac{1}{2}} \geq 1 & (\tilde{\sigma}_{11} < 0) \end{cases}
\tag{47}
$$

i) Transverse direction 2,

$$F_f = \begin{cases} \left[\left(\frac{\tilde{\sigma_{22}}}{Y_T} \right)^2 + \alpha.\left(\frac{\tilde{\sigma_{12}}}{S} \right)^2 \right]^{\frac{1}{2}} \geq 1 & (\tilde{\sigma_{22}} > 0) \\ \\ \left[\left(\frac{\tilde{\sigma_{22}}}{Y_C} \right)^2 + \alpha.\left(\frac{\tilde{\sigma_{12}}}{S} \right)^2 \right]^{\frac{1}{2}} \geq 1 & (\tilde{\sigma_{22}} < 0) \end{cases} \tag{48}$$

where the shear contribution factor α ranges from 0 to 1.

0.4.4   Types of damage evolution

Once damage is initiated in a material point of composite material, the material property must be degraded. This results in strain-softening of the composite materials rather than strain hardening which is observed in conventional materials like metals. A number of post-damage models are proposed for progressive failure analysis and most of them belong to one of the following categories: instantaneous unloading, gradual loading, or constant stress at failure material point as shown in Fig.(12)

Since continuum damage mechanics is a more accurate methodology to predict the failure behaviour of composites, non-linear gradual unloading of the composite material is adopted and simulated in this work. Therefore non-linear material properties degradation model is implemented in this work. Based on the type of damage variable chosen i.e., scalar, vector or 2nd order tensor the damage modelling can be classified into isotropic or anisotropic damage modelling. A brief description about the types of damage modelling, damage evolution equation used and material tangent stiffness etc., is given below
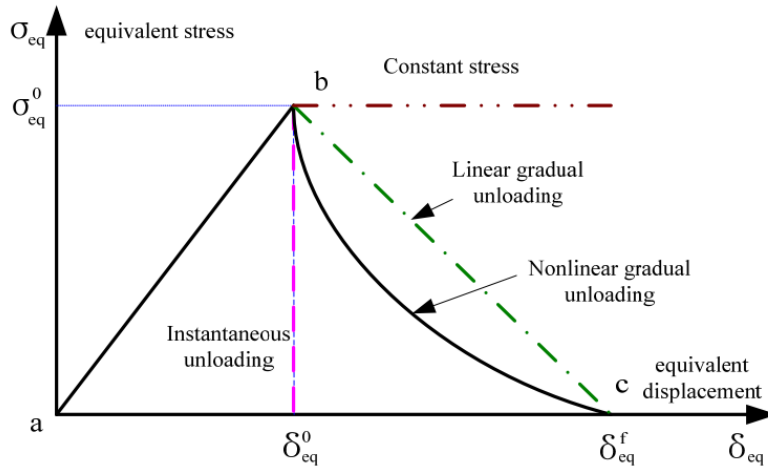
Figure 12: Types of degradation behaviour in damaged composite materials

Isotropic damage

In case of isotropic distribution of cracks, the damage state is usually considered to be isotropic and only a scalar variable D is required to represent the damage state of the material. In this work, a damage evolution law of following form is considered for calculating damage, once the damage has initiated.

$$D \;=\; 1 - e^{-P(\tilde{\epsilon}-k)} \qquad\qquad (49)$$

where P is the softening parameter which determines slope of the damage evolution, $\tilde{\epsilon}$ is 1D equivalent strain and k is the threshold value. Since the Eqn.(49) is an exponential equation, the damage D evolves exponentially from 0 to 1 and the strain-softening will be an exponential decay function. Once the damage starts to evolve the material property must be degraded. Therefore the material stiffness matrix of the damaged material is given by,

$$\mathbb{C}(D) \; = \; (1 - D)\mathbb{C}_0 \tag{50}$$

where $\mathbb{C}_0$ is the material stiffness matrix of the undamaged material. Therefore the stress-strain relation for a strain softening model is given by,

$$\sigma \; = \; \mathbb{C}(D) : \epsilon \tag{51}$$

The finite element equations obtained for strain-softening model is non-linear and therefore Newton-Raphson technique is used to solve the resulting system of non-linear equations. To ensure the robustness of the Newton-Raphson method, it is important to compute the material tangent constitutive tensor $\mathbb{C}_T$. It can be derived as follows,

$$\mathbb{C}_T \; = \; \frac{\partial \sigma}{\partial \epsilon}$$

$$\sigma \; = \; f(\epsilon, D)$$

$$\mathbb{C}_T \; = \; \mathbb{C}(D) + \left(- \mathbb{C}_0 : \epsilon \otimes \frac{\partial D}{\partial \epsilon} \right) \tag{52}$$

In the above equation, the first term $\mathbb{C}(D)$ is the damaged elasticity matrix and second term is due increased damage. In the absence of damage propagation in an increment(For eg., during unloading), the material tangent tensor is equal to the damaged elasticity matrix, so the response is linearly elastic.

Anisotropic damage

In case of orthotropic materials, the material property changes in mutually orthogonal direction. Therefore it is more appropriate to chose a second order damage tensor. In this work, a symmetric second order tensor $\underline{D}$ is chosen , whose principal directions are assumed to coincide with the principal material directions. The eigen values of the damage tensor $\underline{D}$ have a simple physical interpretation i.e., the ith eigen value d_i represents the effective fractional reduction in load carrying area on planes that are perpendicular to i^{th} principal material direction. The damage tensor $\underline{D}$ can

be represented as,

$$\underline{D} = \begin{bmatrix} d_1 & 0 & 0 \\ 0 & d_2 & 0 \\ 0 & 0 & d_3 \end{bmatrix}$$

The relationship between damaged and undamaged material can be established in different way which helps us derive the constitutive equation (i.e.,damaged elastic stiffness matrix) for the damaged material. In this work, hypothesis of strain energy equivalence (Section.0.2.8) and hypothesis of strain equivalence (Section.0.2.7) are used to derive the elastic stiffness matrix of the damaged material. According to hypothesis of strain energy equivalence, from Eqn.(36) the elastic stiffness matrix of the damaged material can be derived as,

$$\mathbb{C}(D) = \mathbb{M}^{-1} : \mathbb{C}_0 : \mathbb{M}^{T,-1} \tag{53}$$

where $\mathbb{M}$ is the damage effect tensor from Section.(0.2.6).

According to hypothesis of strain equivalence, from Eqn.(27) the elastic stiffness matrix of the damaged material can be derived as,

$$\mathbb{C}(D) = \mathbb{M}^{-1} : \mathbb{C}_0 \tag{54}$$

A simple damage evolution law for each principal material direction in case of anisotropic damage is given as follows,

$$d_i = 1 - \frac{e^{-P(F_I - 1)}}{F_I} \tag{55}$$

where d_i (i = 1,2,3) and F_I (I = f,m,z) are damage evolution and failure index in each principal material direction respectively. The material tangent stiffness tensor for anisotropic damage can also be derived in the same way as isotropic damage and it is given as follows

$$\mathbb{C}_T = \frac{\partial \sigma}{\partial \epsilon}$$

$$\sigma = f(\epsilon, \underline{D})$$

$$\mathbb{C}_T = \mathbb{C}(D) + \sum_{i=1}^{3} \left(\frac{\partial \mathbb{C}(D)}{\partial d_i} : \epsilon \otimes \frac{\partial d_i}{\partial \epsilon} \right) \tag{56}$$

In the above equation, the second term(i.e., due to increased damage) must be computed only if the corresponding failure mode is active. Since the damage evolution equation d_i depends on failure index, the term $\frac{\partial d_i}{\partial \epsilon}$ must be computed based on whether the damage happened during tension or compression.

0.4.5   Localisation and Mesh Regularisation

Finite element simulations which uses continuum damage models are susceptible to mesh dependency: when the finite element discretization is refined, the numerical problems does not converge to a physically meaningful solution of the problem. When the material exhibits softening behaviour, which leads to strain localization and this formulation results in a strong mesh dependency i.e., the solution is non-objective with respective to mesh refinement and the energy dissipated decreases with the decrease in finite element size. Merely improving the numerical solution schemes cannot alleviate the problem associated to mesh dependency and localisation. Even if the convergence to the actual solution is improved, the solution may not even make sense from physical point of view. Therefore the so called fracture energy approach is adopted in which fracture energy is included in the damage evolution equation in order to deal with the mesh dependency problem. In this approach the fracture energy of each element is preserved by including the characteristic length (L_c) of the element also in the damage evolution equation. The damage evolution equations based on fracture energy approach for each principal directions is shown below

In Longitudinal direction 1,

$$d_1 = 1 - \frac{e^{P_1(F_f - 1)}}{F_f} \tag{57}$$

In transverse direction 2,

$$d_2 = 1 - \frac{e^{P_2(F_m - 1))}}{F_m} \tag{58}$$

In transverse direction 3,

$$d_3 = 1 - \frac{e^{P_3(F_z - 1)}}{F_z} \tag{59}$$

where $P_1 = \frac{-\sigma_{11}^f \epsilon_{11}^f L_c}{G_{c,1}}$, $P_2 = \frac{-\sigma_{22}^f \epsilon_{22}^f L_c}{G_{c,2}}$ and $P_3 = \frac{-\sigma_{33}^f \epsilon_{33}^f L_c}{G_{c,3}}$

0.4.6   Numerical implementation of the damage model in AN-SYS

As discussed before, the material models necessary for simulating progressive damage failure is implemented using the ANSYS user programmable feature called USERMAT. The damage model implemented using USERMAT computes and updates the current stress and consistent tangent stiffness. The following sections deal

with the numerical implementation of the damage model based on two different methods or criteria used to predict the damage initiation

- Strain based damage model

- Stress based damage model

Strain based damage model

In case of strain based damage model, the damage initiation is predicted using current strain (ϵ_{n+1}). The USERMAT receives strains, stresses and state variables at the beginning of the time increment and the current strain increment. The following steps describe the process of implementing the damage model

- Calculate current strain

$$\underline{\epsilon}_{n+1} = \underline{\epsilon}_n + \underline{\Delta\epsilon}$$

- Calculate the current degraded material stiffness matrix $\mathbb{C}(\underline{D}_n)$

- Calculate the failure indices $F_I(\underline{\epsilon})$

  Check if $F_I \geq F_I\text{max}$

- if $F_I(\underline{\epsilon}) < 1$

$$\underline{\sigma}_{n+1} = \mathbb{C}(\underline{D}_n) : \underline{\epsilon}_{n+1}$$

$$\mathbb{C}_T = \mathbb{C}(\underline{D}_n)$$

- else

  Calculate the damage variables using damage evolution law

$$d_1(F_f), \ d_2(F_m), \ d_3(F_z)$$

  Check if $d_i \geq 0$

  Calculate the updated degraded stiffness based on damage variables

$$\mathbb{C}(\underline{D}_{n+1})$$

  Calculate current stress

$$\underline{\sigma}_{n+1} = \mathbb{C}(\underline{D}_{n+1}) : \underline{\epsilon}_{n+1}$$

  Calculate tangent stiffness

$$\mathbb{C}_T = \mathbb{C}(D) + \sum_{i=1}^{3} \left(\frac{\partial \mathbb{C}(D)}{\partial d_i} : \epsilon \otimes \frac{\partial d_i}{\partial \epsilon} \right)$$

Stress based damage model

In case of stress based damage model, the damage initiation is predicted using effective ($\underline{\tilde{\sigma}}_{n+1}$). The USERMAT receives strains, stresses and state variables at the beginning of the time increment and the current strain increment. The following steps describe the process of implementing the damage model

- Calculate the elastic stiffness matrix $\mathbb{C}$

- Calculate effective stress
$$\underline{\tilde{\sigma}}_{n+1} = \mathbb{C}_0 : \underline{\epsilon}_{n+1}$$

- Calculate the failure indices $F_I(\underline{\sigma})$

    Check if $F_I \geq F_I\text{max}$

- if $F_I(\underline{\sigma}) < 1$
$$\underline{\sigma}_{n+1} = \underline{\tilde{\sigma}}_{n+1}$$

$$\mathbb{C}_T = \mathbb{C}$$

- else

    Calculate the damage variables using damage evolution law

    $$d_1(F_f), \ d_2(F_m), \ d_3(F_z)$$

    Check if $d_i \geq 0$

    Calculate the updated degraded stiffness based on damage variables

    $$\mathbb{C}(\underline{D}_{n+1})$$

    Calculate current stress

    $$\underline{\sigma}_{n+1} = M(D)^{-1} : \underline{\tilde{\sigma}}_{n+1}$$

    Calculate tangent stiffness

    $$\mathbb{C}_T = \mathbb{C}(D) + \sum_{i=1}^{3} \left(\frac{\partial \mathbb{C}(D)}{\partial d_i} : \epsilon \otimes \frac{\partial d_i}{\partial \epsilon} \right)$$

Apply increment $\Delta\epsilon$

$$\underline{\epsilon}_{n+1} \;=\; \underline{\epsilon}_n \,+\, \underline{\Delta\epsilon}$$
$$\underline{\tilde{\sigma}}_{n+1} \;=\; \mathbb{C}_0 \,:\, \underline{\epsilon}_{n+1}$$

Failure Criteria
$(F_I(\underline{\epsilon}))$ or $F_I(\underline{\sigma}))$

Damage onset?

no

yes

Calculate damage variables

Material constitutive equations

$$\underline{\sigma}_{n+1} \;=\; \mathbb{C}(D) \,:\, \underline{\epsilon}_{n+1}$$
(or)
$$\underline{\sigma}_{n+1} \;=\; M(D)^{-1} \,:\, \underline{\tilde{\sigma}}_{n+1}$$
$$C_T \;=\; \frac{\partial\Delta\sigma}{\partial\Delta\epsilon}$$

ANSYS solver

Converged?

yes

no

Next increment until failure or end of analysis

Do for each integration point

Iterate until convergence
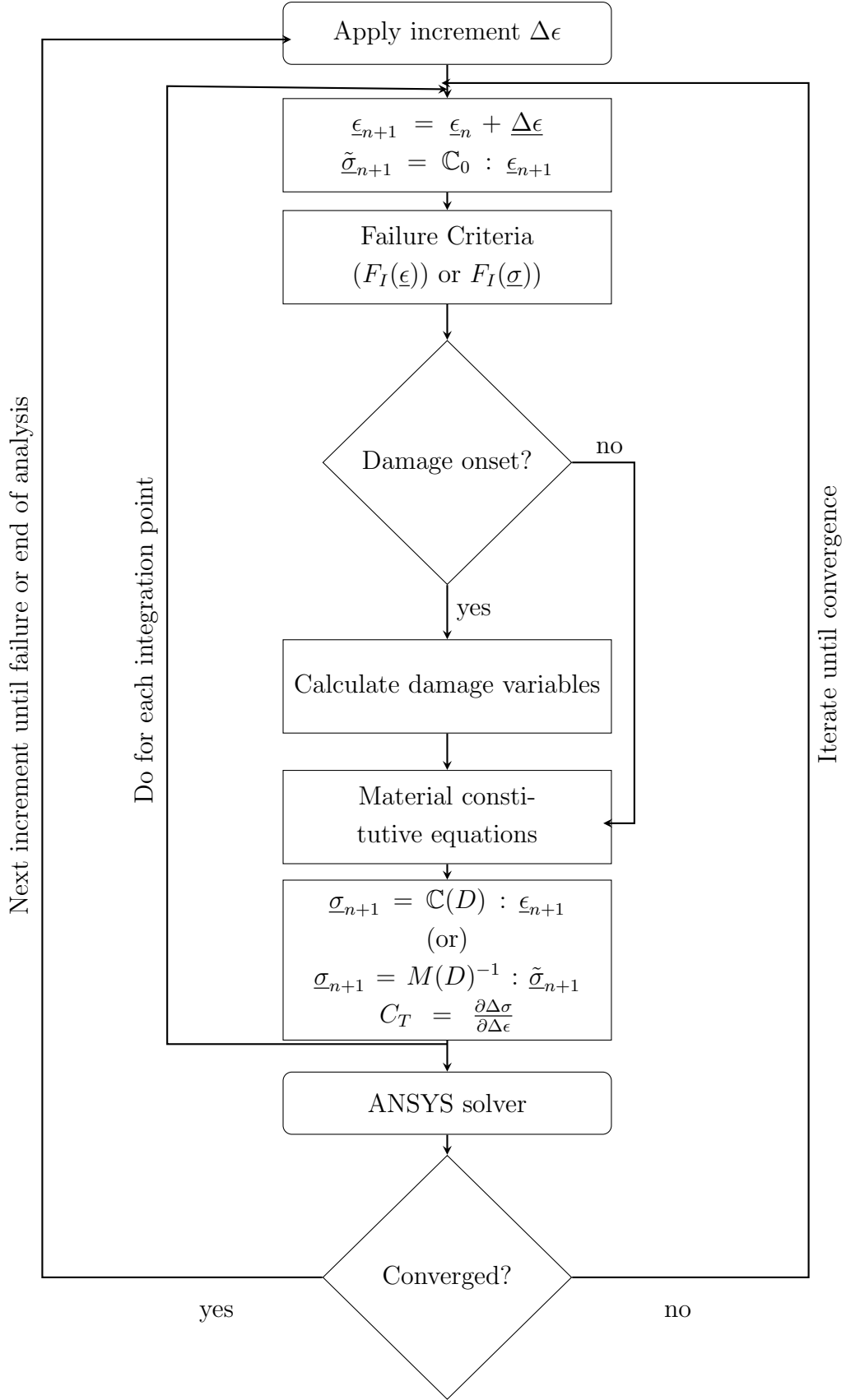
0.5 Results and Discussion

0.5.1 Modelling Linear elastic behaviour of orthotropic materials

Before implementing the damage behaviour in orthotropic materials, their linear elastic behaviour must implemented which demonstrates what happens before the damage initiation. As mentioned before orthtoropic materials are special class of material whose properties change in mutually perpendicular directions. Therefore 9 independent material constants are required in order to model their elastic behaviour numerically. Table (3) summarises the utilised material parameters. The constitutive matrix given in the section(0.2.9) and Hooke's law helps us model the elastic behaviour of the orthotropic materials.

The linear elastic behaviour of the orthotropic material is implemented in
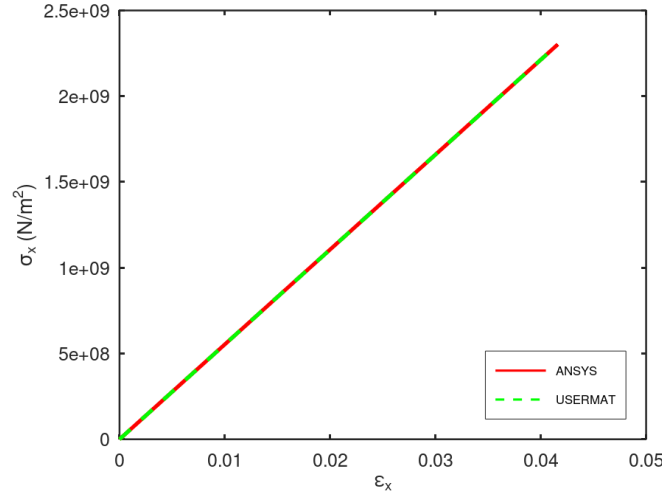
Figure 13: Stress-Strain relation (ANSYS vs USERMAT)

the USERMAT using constitutive equations and in this section the results obtained are compared against the default orthortropic material option present in ANSYS using a structural example. A bar of length 10mm and area $1mm^2$ (b = 1mm, t =1mm) fixed at one end is chosen for the analysis. The bar is constructed using 8 node SOLID

185 elements and full integration has been used. A displacement of 1mm is applied at the free end and the results obtained using the ANSYS default and the USERMAT are presented below. The figure(13) compares the stress-strain relation of the bar obtained using both ANSYS default and USERMAT

Symbol	Material Parameter	Value
E_1	Longitudinal (fibre dominated) elastic modulus	55000e6 N/m^2
$E_2 = E_3$	Transverse(matrix dominated) elastic modulus	9500e6 N/m^2
$\nu_{12} = \nu_{13}$	Poisson's ratio (in-plane)	0.33
ν_{23}	Poisson's ratio (Planes 2-3)	0.27
$G_{12} = G_{13}$	In-plane shear modulus	5500e6 N/m^2
G_{23}	Shear modulus (Planes 2-3)	3000e6 N/m^2
X_t	Longitudinal (fibre dominated) Tensile strength	2500e6 N/m^2
X_c	Longitudinal (fibre dominated) Compressive strength	-2000e6 N/m^2
Y_t	Transverse (matrix dominated) Tensile strength	50e6 N/m^2
Y_c	Transverse (matrix dominated) Compressive strength	-200e6 N/m^2
S_{12}	In-plane strength	50e6 N/m^2

Table 3: Material parameters(Integration point studies)
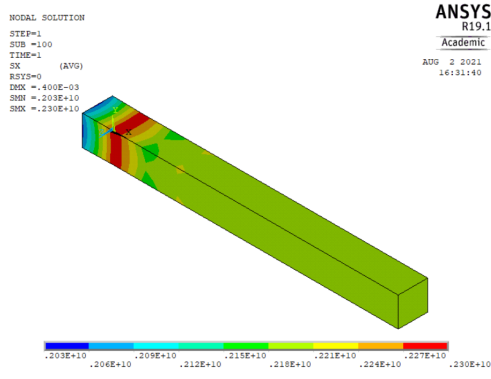
(a) X Component of Stress
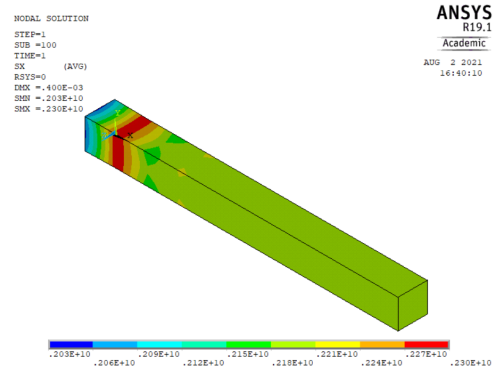
(b) X Component of Stress
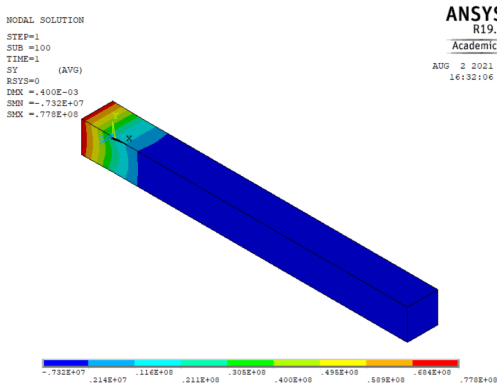
(c) Y Component of Stress
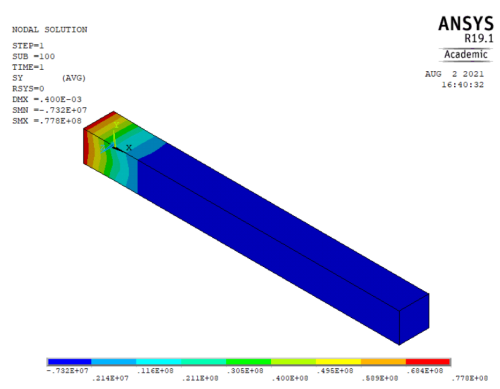
(d) Y Component of Stress

Figure (**??**) and (14) shows the contour plots of the normal stresses (σ_{xx}, σ_{yy} and σ_{zz}) computed using ANSYS default and USERMAT respectively. The comparison of the stress-strain relation and contour plots between the ANSYS default and USERMAT confirms that the results obtained using both options are same and therefore further damage-intiation and damage-evolution processes can now be implemented.

Damage behaviour at integration point level

The material subroutines are first developed on octave and tested using constitutive driver routines which enables us to understand the phenomenon that happens at integration point level. In order to demonstrate the evolution of damage after damage initiation and the strain softening following simple loading cases are investigated at the integration point level.

- Uniaxial tension

- Biaxial tension

- Triaxial tension.
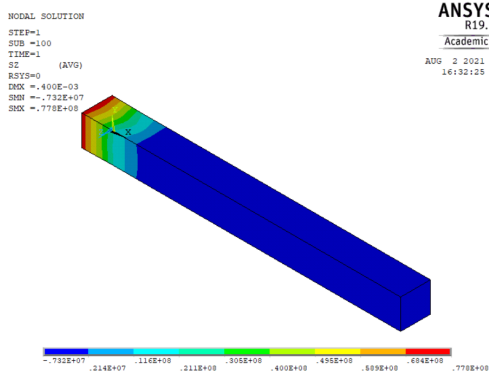
(e) Z Component of Stress
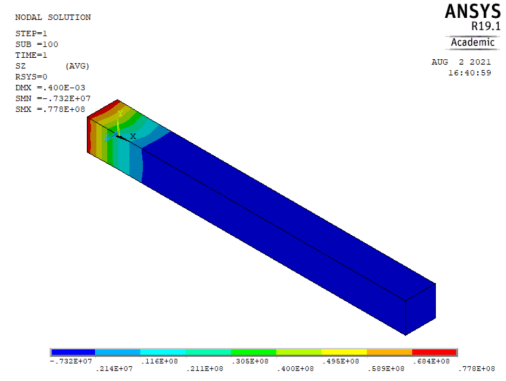
(f) Z Component of Stress

Figure 14: Contour plots of the stress components σ_{xx},σ_{yy} and σ_{zz} of the bar obtained using ANSYS and USERMAT

After that, the material subroutines are implemented in USERMAT and tested in ANSYS environment using a 3D finite element of unit length. The finite element is subjected to the above loading cases and the results are compared against the octave implementation

0.5.2 Uniaxial tension

In case of uniaxial tension the normal stress is present only in one direction and the shear stresses are zero i.e., only one component(diagonal) of the stress tensor is non-zero. In Ansys environment, uniaxial tension is achieved by applying a displacement on the finite element in a normal direction (11) which increases the strain ϵ_{11} linearly and the lateral(transverse) contraction is not constrained. 3D Hashin's quadratic strain criteria (Section(0.4.3)) is used to predict the damage initiation and exponential damage evolution law (Eqn(55)) is used to calculate the damage evolution. The results obtained from Ansys and usermat are presented in the Figure(15a) and (15b) respectively. The figure (15c) shows the evolution of damage variables. The system is linearly elastic till the damage initiation strain and the damage is zero. Once the strain ϵ_{11} exceeds the damage initiation strain, the damage d_1 starts to evolve exponentially and the stress starts to drop due to reduction in stiffness in 11 direction. The damage variables d_2 and d_3 are zero. The comparison between the figures (15a) and (15b) suggests that the material routine implemented in octave and usermat are numerically similiar to each other.

The scalar softening parameter(P) in the damage evolution equation(55) determines the slope of the damage curve. The following figure demonstrates the influence of the softening parameter (P) in the damage evolution
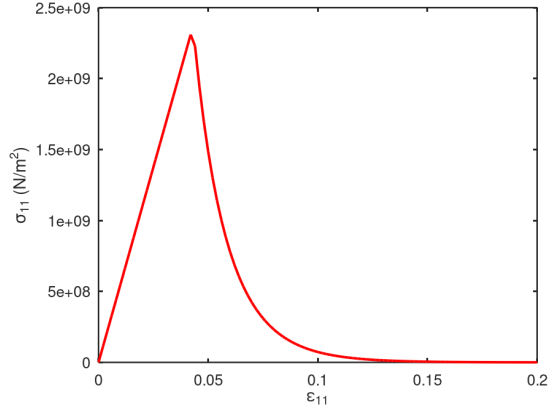
44

(a) Stress-Strain relation (ANSYS)
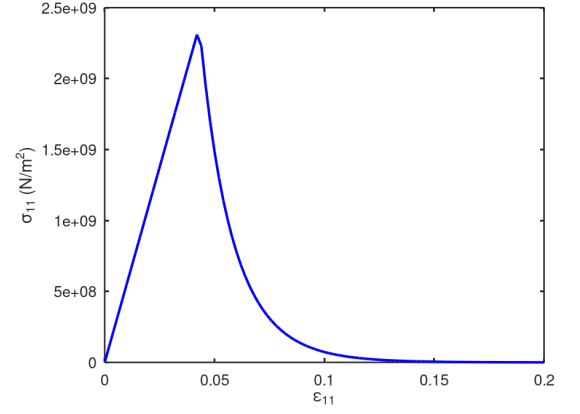
(b) Stress-Strain relation (Octave)
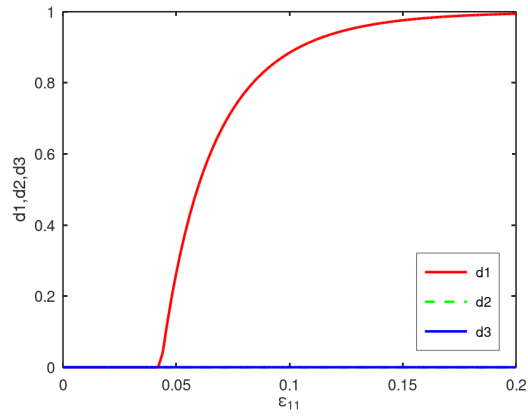
(c) Evolution of damage

Figure 15: Evolution of stress and damage components for a uniaxial tension test in 11 direction
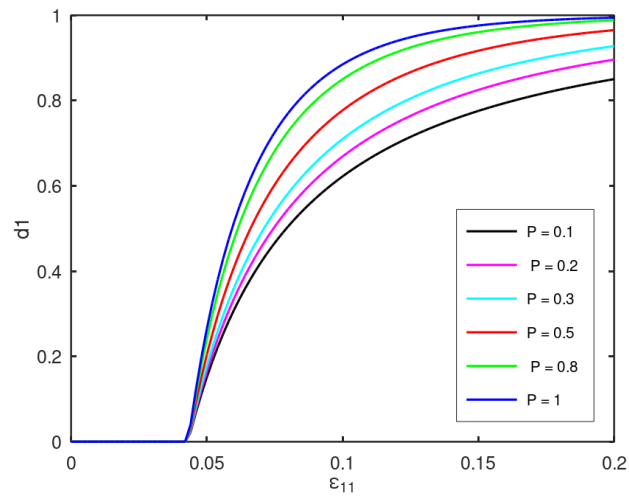

Figure 16: Influence of softening parameter P in the damage evolution)

Drawbacks of strain based damage initiation criteria

Since the lateral contraction is not constrained during uniaxial tension, the transverse directions experience compression due to poisson's effect i.e., ϵ_{22} and ϵ_{33} will be negative. If the compressive strength of transverse directions 2 and 3 are sufficiently low, the strains ϵ_{22} and ϵ_{33} will exceed the damage initiation strain. This leads to damage evolution without the presence of stress in transverse directions 2 and 3. This phenomenon cause convergence issues and the model stops when the damage d_2 or d_3 evolve without the presence of stress. The image (17) shows the convergence issue and the failure of the model to run when the damage d_2 starts when using strain-based damage initiation criteria

```
d1 = 0
d2 = 0.025175
d3 = 0
d1 = 0
d2 = 0.025176
d3 = 0
d1 = 0
d2 = 0.025176
d3 = 0
d1 = 0
d2 = 0.025176
d3 = 0
d1 = 0
d2 = 0.025176
d3 = 0
|sbar| = 3587307.3414
error: No convergence after 100 global iterations
error: called from
    drive at line 96 column 13
```

Figure 17: Convergence error due to evolution of damage d_2 without the presence of stress

This problem can be rectified by using stress-based damage initiation criteria. Since damage evolution depends on failure index F, the transverse failure indices F_m and F_z will be zero during uniaxial tension if the stress based damage initiation criteria is used. This results in zero damage in transverse direction. The following section presents the results obtained using stress-based damage initiation and the use of mesh regularisation in the damage evolution law.

Stress based damage initiation and mesh regularisation

As mentioned in the section (0.4.5), the strain localisation problems results in strong mesh dependency so fracture energy and characteristic length(L_c) of the element has to been included in the damage evolution law in order to alleviate the problem. So the material routine is modified by changing the damage initiation criteria to maximum stress criteria(2) and including the damage evolution equations from (57) to (59). The uniaxial tension is conducted again with the above mentioned changes and with very low transverse compression strength and the results are presented below From figure (18c) it is evident that the damage d_2 and d_3 are zero as a result of stress-based damage initiation because the stress components σ_{22} and σ_{33} are zero under uniaxial tension. While using mesh regularisation, the slope of the damage curve is determined by the characteristic length (L_c) which depends on the volume of the element. The following
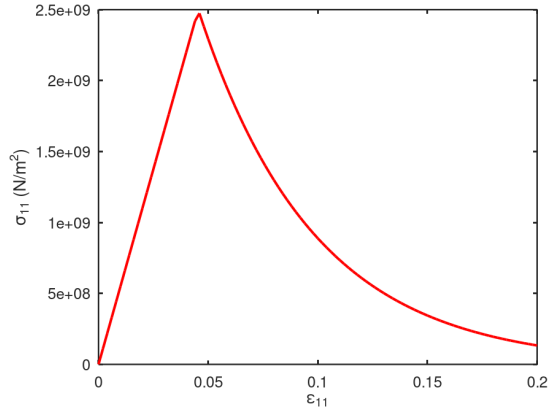
(a) Stress-Strain relation (ANSYS)
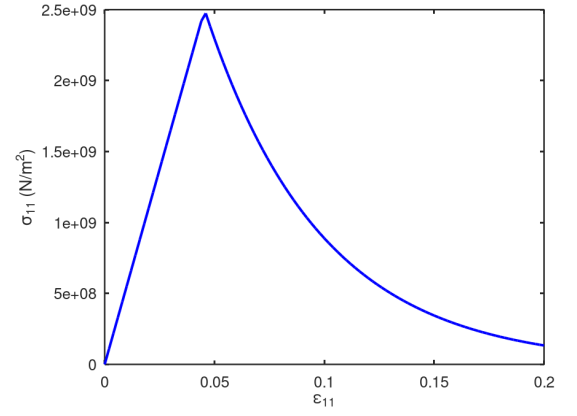
(b) Stress-Strain relation (Octave)
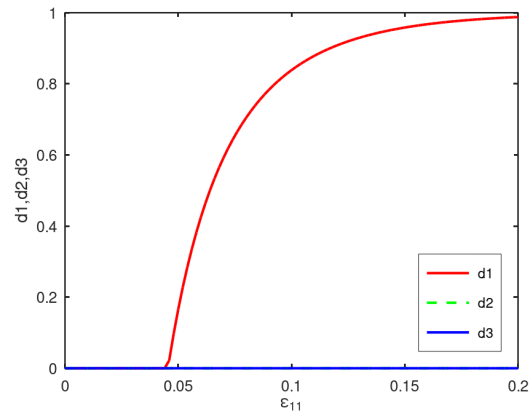
(c) Evolution of damage

Figure 18: Evolution of stress and damage components with stress-based damage initiation criteria under uniaxial tension

47

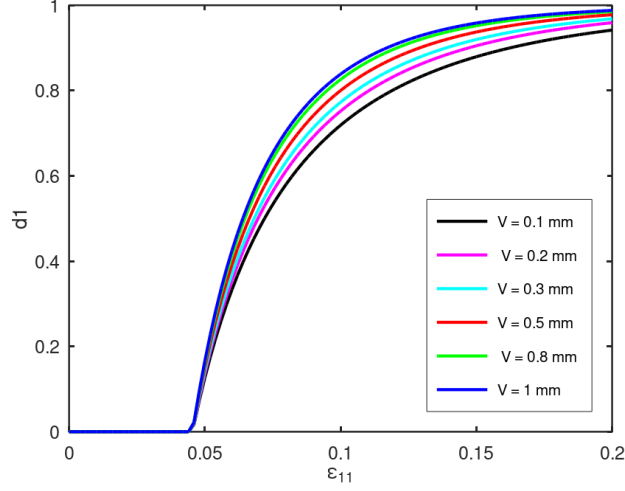figure (16) shows how the damage evolution is affected by the volume of the element,

Figure 19: Influence of element volume (V) in the damage evolution

Discussion about tangent stiffness

In case of uniaxial tension the components of the stress tensor other than σ_{11} are zero. Since stress-conditions are enforced, the octave driver routine uses Newton-raphson method to determine the input strain components other than ϵ_{11} iteratively. The Newton-raphson method requires tangent stiffness for computation which can be derived using the equation (56) for anisotropic damage. This enables us to test the derived algorithmic tangent stiffness (ATS) before implementing it in USERMAT which is then used by Ansys for solving non-linear system of equations which arise due to strain softening. The derived algorithmic tangent stiffness is verified by comparing it with the numerical tangent stiffness computed using numerical perturbation. In numerical perturbation, the coefficients of strain tensor are perturbed by a very small value i.e., $\Delta\epsilon_{kl}^{n+1} = \delta$ (where $\delta \ll 1$) and the resulting stress perturbations are calculated.

$$\Delta\sigma_{ij}^{n+1} = \sigma_{ij}^{n+1}(\epsilon_{kl}^{n+1} + \delta) - \sigma_{ij}^{n+1}(\epsilon_{kl}^{n+1}) \tag{60}$$

Then the components of the tangent stiffness tensor can be estimated as

$$C_T = \frac{\Delta\sigma_{ij}^{n+1}}{\Delta\epsilon_{kl}^{n+1}} \tag{61}$$

Since the material routine must be evaluated for every perturbation of ϵ_{kl} the routine has to be called six time recursively per load-step iteration. The figure (20a) and (20b) shows the strain components ϵ_{22} and ϵ_{33} computed using algorithmic and numerical tangent stiffness which are plotted against ϵ_{11} respectively.

These comparison between above plots clearly indicates that the tangent stiffness
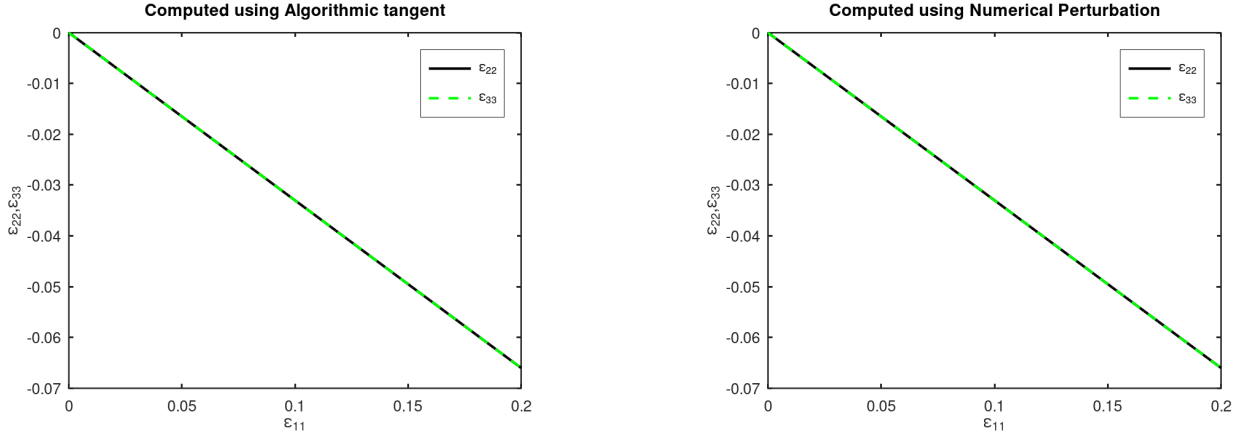
(a) $\epsilon_{22}, \epsilon_{33}$ vs ϵ_{11} (Algorithmic tangent)

(b) $\epsilon_{22}, \epsilon_{33}$ vs ϵ_{11} (Numerical perturbation)

Figure 20: The Strain components ϵ_{22} and ϵ_{33} computed using algorithmic and numerical tangent stiffness under uniaxial tension

computed using algorithmic tangent and numerical tangent are numerically similar to each other.

0.5.3 Biaxial tension

In case of biaxial tension, normal stresses are present only in two normal directions and all the shear stresses are zero i.e., only two components(diagonal) of the stress tensor are non-zero. In Ansys, biaxial tension is achieved by applying same displacements in two normal directions of the finite element (11 and 22 direction) and the contraction in 3rd direction (33) is unconstrained. The following figures shows the corresponding stress and damage components obtained from the test. Since the tensile strength in transverse direction is very low compared to the longitudinal direction, evolution of damage (d_2) begins very soon and simultaneously the stress component (σ_{22}) drops as seen in figures (21c) and (21d).
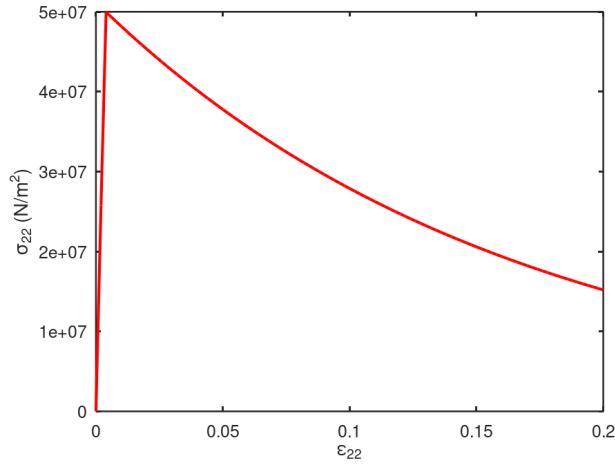
Triaxial tension

In case of triaxial tension, the normal stresses are present in all three normal directions and all the shear stresses are zero i.e., only diagonal components of the stress tensor are non-zero. In Ansys, triaxial tension is achieved by applying same displacement in all three normal directions (11, 22 and 33 direction). The following figures shows the corresponding stress and damage components obtained from the test
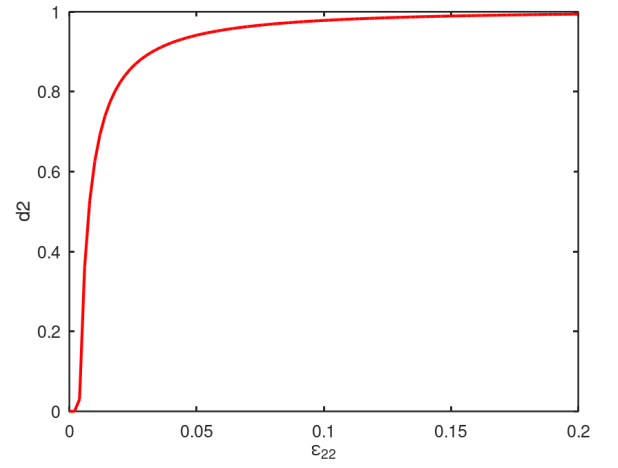
(a) σ_{11} vs ϵ_{11}
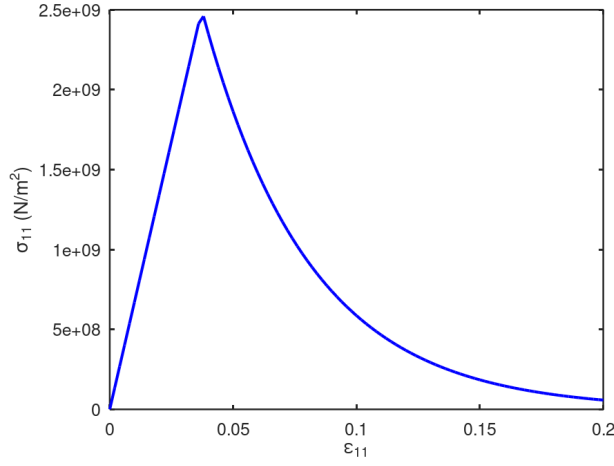
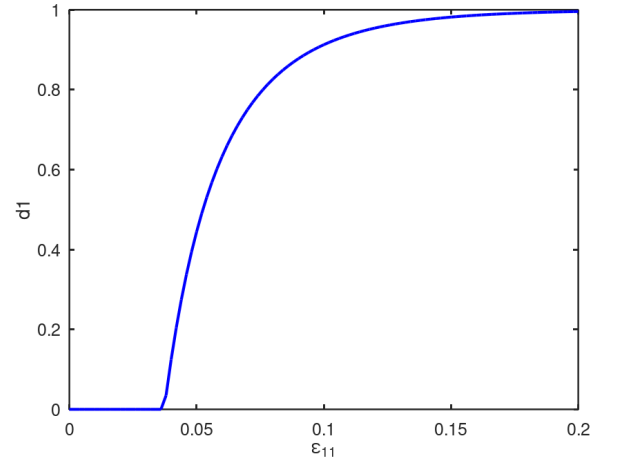(b) Evolution of damage d_1

(c) σ_{22} vs ϵ_{22}
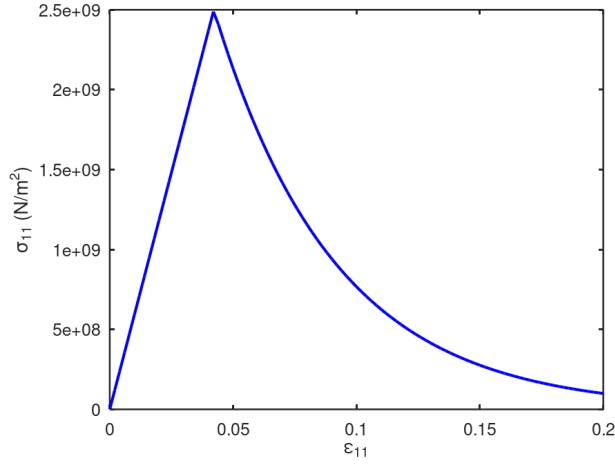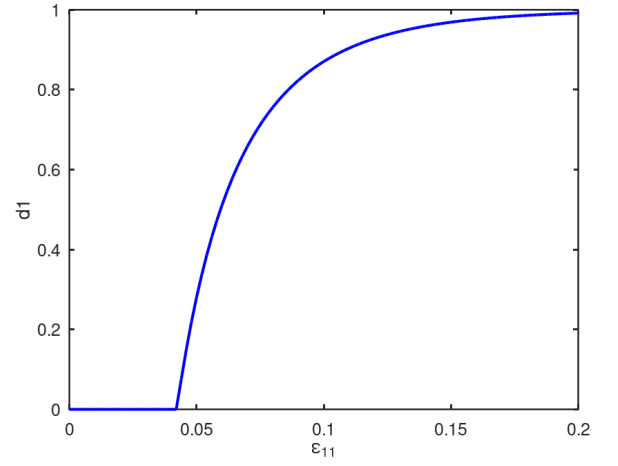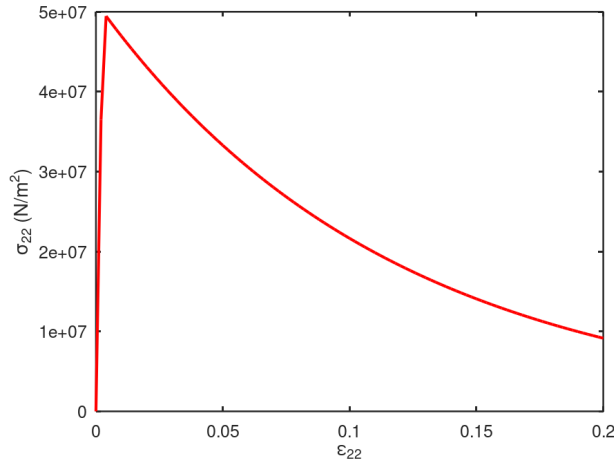
(d) Evolution of damage d_2

Figure 21: Evolution of stress and corresponding damage components under biaxial tension

(a) σ_{11} vs ϵ_{11}
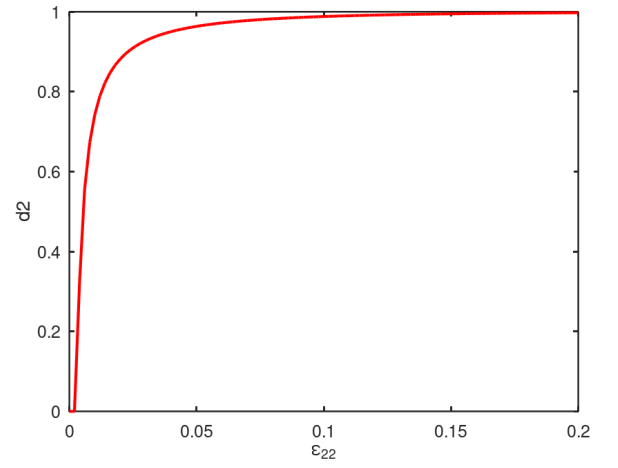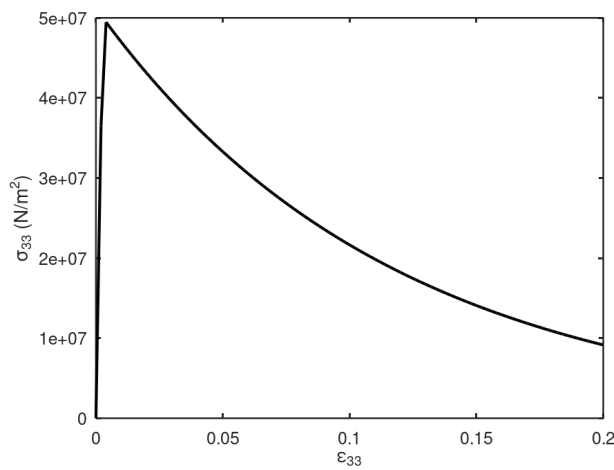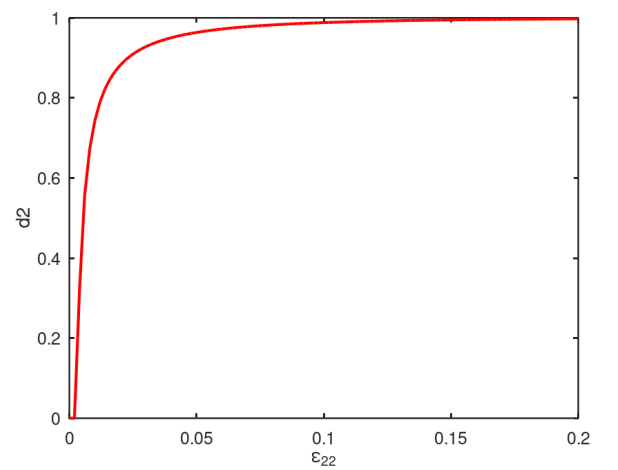
(b) Evolution of damage d_1

(c) σ_{22} vs ϵ_{22}

(d) Evolution of damage d_2

(e) σ_{33} vs ϵ_{33}

(f) Evolution of damage d_3

Figure 22: Evolution of stress and corresponding damage components under triaxial tension

Since the material properties are same in 22 and 33 direction and the tensile strength is very low compared to the longitudinal direction, the damage d_2 and d_3 evolves simultaneously (Fig (22d) and (22f)) and very soon as expected. Therefore the stress components σ_{22} and σ_{33} drops very soon as shown in the figure (22c) and (22e)